# HYBRID VOLTAGE SAG MITIGATION FOR RENEWABLE INTEGRATED WEAK DISTRIBUTION SYSTEMS USING A LOAD MANAGEMENT AND ROBUST INVERTER CONTROL APPROACH

Kurukulasuriya Tharindu Stephan Fernando

(218945K)

Degree of Master of Science

Department of Electrical Engineering

University of Moratuwa

Sri Lanka

January 2024

# HYBRID VOLTAGE SAG MITIGATION FOR RENEWABLE INTEGRATED WEAK DISTRIBUTION SYSTEMS USING A LOAD MANAGEMENT AND ROBUST INVERTER CONTROL APPROACH

Kurukulasuriya Tharindu Stephan Fernando

(218945K)

Dissertation submitted in partial fulfilment of the requirements for the degree Master of Science

Department of Electrical Engineering

University of Moratuwa

Sri Lanka

January 2024

# DECLARATION

I declare that this is my own work and this thesis does not incorporate without acknowledgement any material previously submitted for a Degree or Diploma in any other University or institute of higher learning and to the best of my knowledge and belief it does not contain any material previously published or written by another person except where the acknowledgement is made in the text.

Also, I hereby grant to the University of Moratuwa the non-exclusive right to reproduce and distribute my dissertation, in whole or in part in print, electronic or other medium. I retain the right to use this content in whole or part in future works (such as articles or books).

Signature: Date: 28-06-2024

The above candidate has carried out research for the Masters dissertation under my supervision.

Name of Supervisor: Prof.Lidula N.Widanagama Arachchige

Signature of the Supervisor: Date: 28-06-2024

Name of Supervisor: Dr. H. M. Wijekoon Banda

Signature of the Supervisor: Date: 12-07-2024

# DEDICATION

To my parents, my siblings, and my beloved wife

# ACKNOWLEDGEMENT

First and foremost, I extend my sincere gratitude to Prof. Lidula N. Widanagama Arachchige, my internal supervisor, for her unwavering guidance and encouragement during the entire research.

Secondly, I express my sincere appreciation for the support given by my external supervisor, Dr. H. M. Wijekoon Banda. I would like to acknowledge his expertise and guidance, which significantly contributed to the success of this research.

I would like to express my gratitude to the academic staff of the Department of Electrical Engineering, Faculty of Engineering, the University of Moratuwa, Sri Lanka. Their insightful comments and unwavering support during the presentations have been invaluable and greatly appreciated.

I express gratitude to the CEB management for allowing me to use the data. Special thanks to Eng. Dinesh Dissanayake – CE (CPCDP-CEB), Eng. Isuru Kumarasinghe - PM (CPCDP-CEB), Eng. Dimuthu Wijewickrama - EE (CPCDP-CEB), and Eng. Dimalka Karunajeewa - EE (CPCDP-CEB) for their unwavering support.

Finally, I express my heartfelt thanks to my wife, Dr. Omalka Fonseka, my parents, and family members for their understanding and support in numerous ways, enabling me to consistently reach and surpass my research goals.

# ABSTRACT

The world is rapidly transitioning towards renewable energy sources, with Inverter-Based Resources (IBRs) emerging as key power sources for future distribution systems. The electrification of rural and remote areas is progressing rapidly, bringing power to previously underserved locations. However, remote distribution networks face challenges, with one significant issue being lower fault levels.

Weak distribution networks in these remote areas give rise to several problems, with voltage sag being a primary concern. Voltage sag, often caused by sudden changes in load or faults on the grid, poses a particular threat to process controllers, PLCs, variable speed drives, robots, data processing and control equipment, in particular, are highly sensitive to voltage sags, risking potential data loss. The simultaneous operation of large machines can further exacerbate the challenges associated with low fault levels.

In the context of IBR-based distribution systems, vulnerability to unbalanced voltage sag is a specific concern. The Synchronous Reference Frame-Phase Locked Loop (SRF-PLL) may incorrectly estimate the positive sequence voltage component, resulting in a loss of controllability for the three-phase inverter. A grid-connected power converter, in particular, is sensitive to voltage disturbances, as its control system may lose controllability under such distorted operating conditions. This may lead to damage the inverter, as it is unsuitable for injecting unbalanced currents and lacks a specific control loop for negative-sequence current components. The abrupt disconnection of inverters can result in voltage collapse, frequency instability, and synchronous angle instability.

This research has addressed these challenges by developing a voltage sag mitigation technique for weak distribution systems. A robust inverter control system capable of maintaining connectivity during voltage sag events and a pre-assigned priority load management scheme to effectively mitigate voltage sag were designed. Performance evaluation revealed the success in mitigating voltage sag by applying the proposed techniques when integrating IBR to weak grids.

**Keywords**: Inverter-Based Resources, Large Machine Operation, Voltage Sag, Weak Distribution Grid.

# TABLE OF CONTENTS

HYBRID VOLTAGE SAG MITIGATION FOR RENEWABLE INTEGRATED WEAK DISTRIBUTION SYSTEMS USING A LOAD MANAGEMENT AND ROBUST INVERTER CONTROL APPROACH ..... 1

DECLARATION ..... i

DEDICATION ..... ii

ACKNOWLEDGEMENT ..... iii

ABSTRACT ..... iv

Table of Contents ..... v

List of Figures ..... viii

List of Tables ..... x

List of Abbreviations ..... xi

List of Appendices ..... xii

Chapter 1 ..... 1

1. INTRODUCTION ..... 1

Leveraging Inverter-Based Resources for Sustainability ..... 1

Voltage Sag ..... 1

Main Causes of Voltage Sag ..... 2

1.1.1 Connection of Large Inductive Loads ..... 2

1.1.2 Sudden Overloading of Circuits ..... 3

1.1.3 Network Faults ..... 3

Low Fault Level Grid Characteristics ..... 3

1.1.4 Large Inductive Machine Operation ..... 4

1.1.5 Simultaneous Operation of Machines ..... 5

Problem Statement ..... 5

Scope ..... 6

Objectives ..... 6

Chapter 2 ..... 8

2. LITERATURE REVIEW ..... 8

Conventional Phase Locked Loop ..... 8

Conventional Inverter Control System Drawbacks ..... 10

Decoupled Double Synchronous Reference Frame -Phase Locked Loop (DDSRF-PLL) ……..12
Flexible Positive and Negative Sequence Control (FPNSC) ..... 13
Inverter Controller during Voltage Sag ..... 14
Estimation of Over Current Limits ..... 14
Removal of Coupling Effects in DDSRF-PLL ..... 16
Loads Behaviour during Voltage Sag ..... 16
Equipment Sensitivity for Voltage Sag ..... 18
Chapter 3 ..... 21
3. METHODOLOGY ..... 21
General Illustration ..... 21
Chapter 4 ..... 23
4. MODELING APPROACH ..... 23
Inverter Unbalanced Operation ..... 23
4.1.1 Decoupled Double Synchronous Reference Frame -Phase Locked Loop (DDSRF-PLL) ..... 23
4.1.2 Flexible Positive and Negative Sequence Control (FPNSC) ..... 26
Load Management System ..... 26
4.1.3 Sag Detection for Load Management Scheme ..... 26
4.1.4 Load Prioritization Scheme ..... 27
4.1.5 Load Shedding Scheme ..... 31
4.1.6 Typical Response Time ..... 32
4.1.7 Restoration Scheme ..... 33
Integrated System Operation ..... 34
Chapter 5 ..... 36
5. UNBALANCED INVERTER OPERATION ..... 36
Unbalanced Inverter Operation ..... 36
Summary ..... 38
Chapter 6 ..... 39
6. COST OF IMPLEMENTATION ..... 39
Typical Implementation Cost ..... 39
Chapter 7 ..... 41

7. IMPLEMENTATION OF THE PROPOSED METHOD ..... 41
Case Study 1 ..... 41
7.1.1 Summary ..... 45
7.1.2 Techno-Economic Analysis ..... 46
Case Study 2 ..... 48
7.1.3 Load Management Scheme Operation ..... 48
7.1.4 Inverter Unbalanced Operation ..... 51
Chapter 8 ..... 55
8. CONCLUSION ..... 55
Future Improvements ..... 57
9. REFERENCES ..... 59

Appendix - A: ETAP simulation reports for Case Study 1 with various loading on the distribution system

# LIST OF FIGURES

Figure 1-1 Voltage sag due to large machine operation [2] 2

Figure 1-2 Different type of voltage sags due to faults, (a) Three-phase to ground fault through an impedance, (b) Phase to phase fault, (c) Single phase to ground fault, (d) Phase to phase to ground fault. 4

Figure 1-3 Voltage sag change with PCC fault level 5

Figure 2-1 Unbalanced Voltage 9

Figure 2-2 Sequence components of unbalanced voltage [8] 9

Figure 2-3 Phase angle during the unbalanced period [8]. 9

Figure 2-4 Incorrectly analyzed sequence components [8] 10

Figure 2-5 The magnetic flux of 5.5 kW induction motor with 85% rated load. The magnetic flux of normal operation [16] 17

Figure 2-6 The magnetic flux at half cycle since the 30% voltage sag [16]. 18

Figure 2-7 Old CBEMA and ITIC curves [17] 19

Figure 2-8 New ITI (CBEMA) curve (2000) [18] 20

Figure 3-1 Flowchart of Inverter operation mode to mitigate unbalanced voltage sag 21

Figure 3-2 Flowchart of Load Management System 22

Figure 4-1 Positive sequence component during the unbalanced voltage sag 23

Figure 4-2 Negative sequence component during the unbalanced voltage sag 24

Figure 4-3 Grid voltages during unbalance 24

Figure 4-4 Phase angle during the unbalance 25

Figure 4-5 Detected dq signals for the positive sequence component 25

Figure 4-6 Detected dq signals for the negative sequence component 25

Figure 4-7 Block diagram of grid voltage decomposition 26

Figure 4-8 Load management scheme detection technique 27

Figure 4-9 Load prioritization scheme 28

Figure 4-10 Implementation of proposed load management scheme 29

Figure 4-11 Implementation of proposed load management scheme 29

Figure 4-12 Load priority level selector interface 30

Figure 5-1 Unbalanced fault 36

Figure 5-2 Matlab model for the general system 37

Figure 5-3 The unbalance occurrence with absent inverter support 37

Figure 5-4 The unbalance occurrence with inverter support 38

Figure 7-1 ETAP model for case study 1 41

Figure 7-2 Operating a large induction machine within a distribution system under light load condition 42

Figure 7-3 Operating a large induction machine within a distribution system under 50% load condition 42

Figure 7-4 Load management scheme operation 43

Figure 7-5 Load restoration execution 44

Figure 7-6 Without load management scheme 46

Figure 7-7 Geographical view of the distribution system (Location: Pahala Bomiriya) 48

Figure 7-8 Matlab model of the selected distribution system 50

Figure 7-9 Voltage at the load PCC 50

Figure 7-10 Voltage recovery by using the LMS 51

Figure 7-11 Unbalanced fault at the selected distribution system 51

Figure 7-12 Inverter 1 terminal voltage without inverter support 52

Figure 7-13 Phase voltages during the voltage sag with unbalanced support from the inverter 1 52

Figure 7-14 RMS phase voltages during the voltage sag without unbalanced support from the inverter 1 52

Figure 7-15 RMS phase voltages during the voltage sag with unbalanced support from the inverter 1 53

Figure 7-16 Inverter current injection during voltage unbalance 54

# LIST OF TABLES


Table 4-1 Load shedding scheme 32

Table 4-2 Typical latencies of communication protocols [25] 33

Table 4-3 Restoration Plan 33

Table 6-1 Typical System Implementation Component Cost 39

Table 7-1 Load shedding scheme operation 43

Table 7-2 Load restoration execution 44

Table 7-3 Economic analysis for case 1 47

Table 7-4 System data 48

Table 7-5 Consumer details of the selected system 49

# LIST OF ABBREVIATIONS

| Abbreviation | Description |
|---|---|
| DDSRF | Decoupled Double Synchronous Reference Frame |
| PLL | Phase Locked Loop |
| SRF | Synchronous Reference Frame |
| LMS | Load Management Scheme |
| BESS | Battery Energy Storage System |
| IBRs | Inverter Based Resources |
| PLC | Programmable Logic Controllers |
| SCR | Short Circuit Ratio |
| PCC | Point Of Common Coupling |
| AC | Alternative Current |
| DC | Direct Current |
| PWM | Pulse Width Modulation |
| CBEMA | Computer and Business Equipment Manufacturers Association |
| ANSI | American National Standards Institute |
| LVRT | Low Voltage Ride Through |
| FPNSC | Flexible Positive and Negative Sequence Control |
| rms | root mean square |
| HVAC | Heat Ventilation Air Conditioning |
| IoT | Internet of Things |
| MV | Medium Voltage |
| LV | Low Voltage |

# LIST OF APPENDICES


| Appendix | Description |
|---|---|
| Appendix - A | ETAP simulation reports for Case Study 1 with various loading on the distribution system |

# CHAPTER 1

# INTRODUCTION

## Leveraging Inverter-Based Resources for Sustainability

Access to electricity has become a fundamental human need, reaching even the smallest rural communities. Utilities aim to extend beyond urban centres, electrifying remote and rural areas that have long been without access to electricity. These efforts hold the potential for economic growth and improved livelihoods.

As the world moves towards a greener energy landscape, Inverter Based Resources (IBRs) have gained significant attention. Due to the environmental benefits and capacity for sustainable energy generation, IBRs, including solar and wind systems, are emerging as prominent components of distribution systems.

Therefore, the addition of the IBRs makes rural electrification a more attractive option. However, electrification of rural areas often presents unique challenges due to their distance from existing power grids. These areas may be either grid connected or operate with off-grid connections. Due to their distance from generation stations, grid connected locations in such regions often encounter lower fault levels, rendering them susceptible to the challenges associated with weak grids.

One of the main power quality issues is voltage sag. Low voltage ride through and limited inertia of inverter-based resources can exacerbate voltage sags in weak grids. Additionally, IBRs can be vulnerable to unbalanced voltage sags, potentially leading to a loss of controllability.

## Voltage Sag

As defined in IEEE Std 1159-2019, a voltage sag is "a decrease in root-mean-square (rms) voltage (0.1 pu to 0.9 pu) at the power frequency for a duration of 0.5 cycles to 1 minute" [1]. Voltage sag can be defined as a critical power quality challenge encountered by numerous industrial and household customers. This issue significantly affects various process plant systems, including process controllers, Programmable Logic Controllers (PLCs), variable speed drives, and robots. In instances involving

motor starters, a voltage sag can escalate into the failure of relays and contactors, potentially resulting in a complete shutdown of operations.

The sensitivity of data processing and control equipment to voltage sags poses a substantial risk of potential data loss. The systems, which are crucial for seamless operations, are particularly vulnerable to voltage sags. Therefore, addressing voltage sag issues in industrial settings is crucial [3].

## Main Causes of Voltage Sag

The connection of large loads, sudden overloading of circuits and network faults can cause voltage sags. Severity of voltage sag depends on the specific event.

### 1.1.1 Connection of Large Inductive Loads

Connecting a large inductive load increases current draw, causing voltage sags. The severity depends on load size and system strength. Large inductive loads, such as industrial plants, induction motors, and arc furnaces, typically have high inrush currents, which causes shallow voltage sags for longer durations as shown by Figure 1-1 [2].

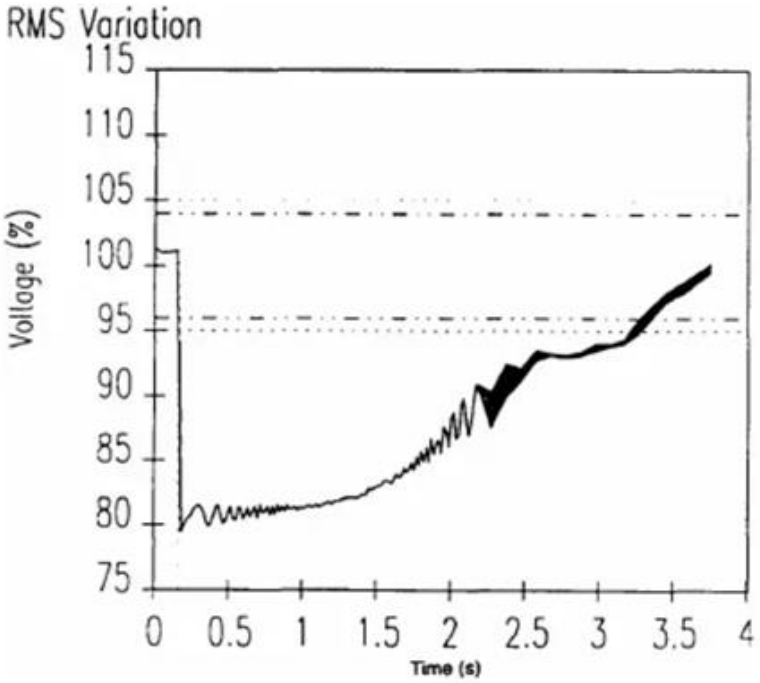


Figure 1-1 Voltage sag due to large machine operation [2]

### 1.1.2 Sudden Overloading of Circuits

Sudden overloading of circuits occurs when more current is drawn from a circuit than it is designed to handle. This can happen when multiple appliances or devices are turned on at the same time, or when a faulty appliance is plugged in.

Sudden circuit overloads can also cause voltage sags, though typically less severe than those caused by large machines starting up [2].

### 1.1.3 Network Faults

In general, faults in transmission systems are quickly cleared compared to those in distribution systems. Transmission systems typically require rapid fault clearance, necessitating fast protection measures. Circuit breakers are used to isolate the fault as quickly as possible. Distance protection and differential protection, common in transmission and sub transmission systems, contribute to quick fault detection and clearance [2].

In contrast, distribution systems typically rely on overcurrent protection, which often involves time grading techniques, leading to longer fault clearing times. An exception exists in systems using current limiting fuses, which can promptly clear faults.

As illustrated in Figure 1-2, the severity and depth of voltage sags depend on the type of fault on the electrical system.

## Low Fault Level Grid Characteristics

A weak grid in a power system refers to a network with a low short circuit ratio (SCR) and inertia constant (H). This means that the system has limited capacity to handle sudden changes in loads, leading to voltage and frequency variation [4].

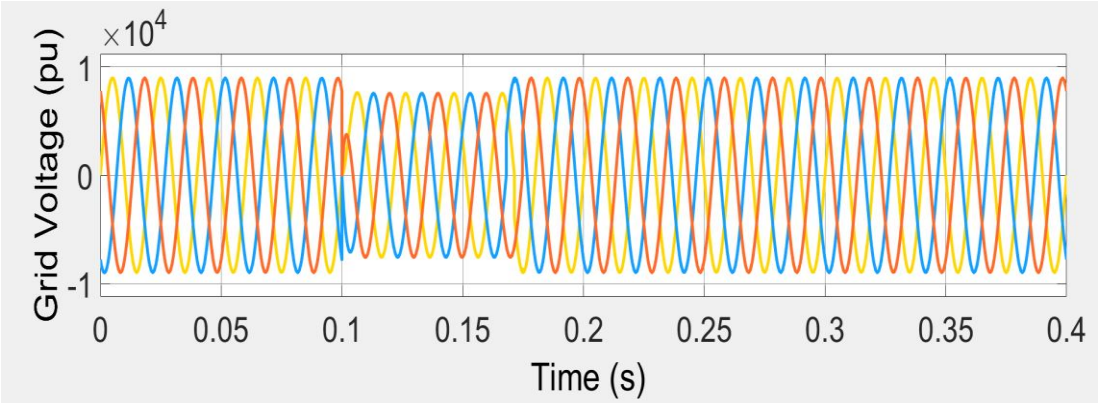


a)

b)

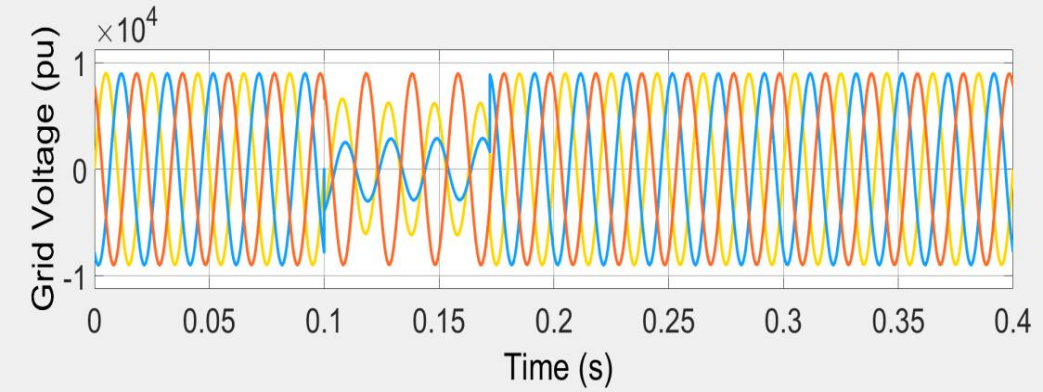


c)

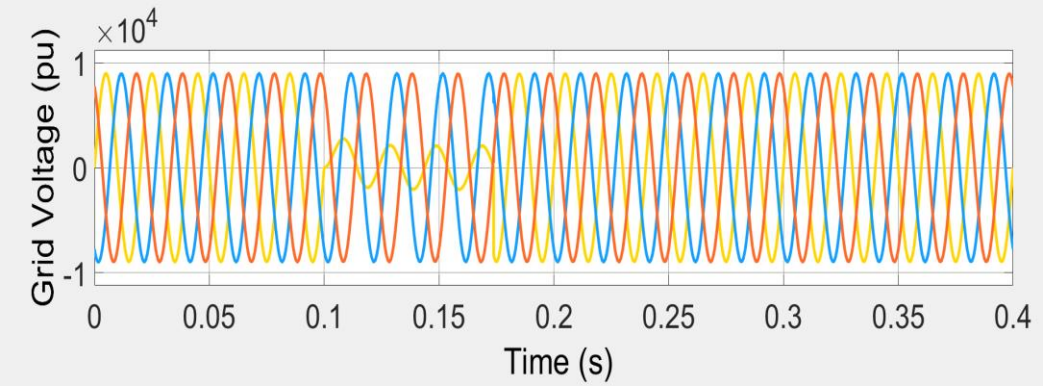


d)

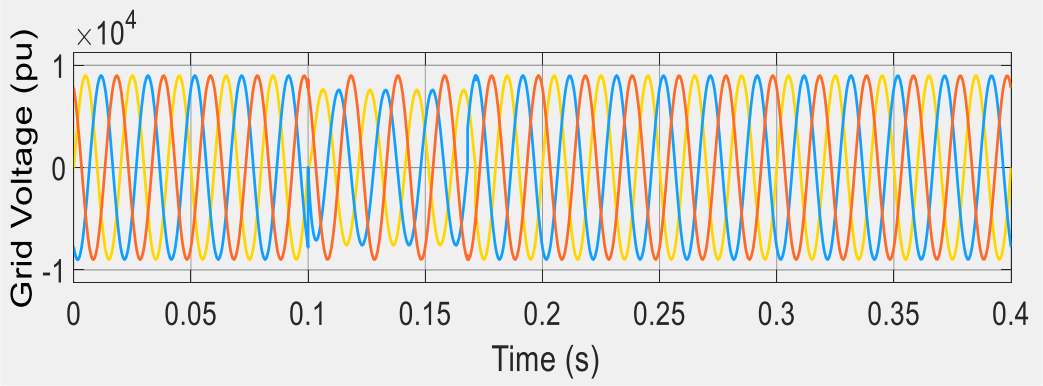


Figure 1-2 Different type of voltage sags due to faults, (a) Three-phase to ground fault through an impedance, (b) Phase to phase fault, (c) Single phase to ground fault, (d) Phase to phase to ground fault.

### 1.1.4 Large Inductive Machine Operation

The operation of large machines within a weak grid introduces several technical considerations. Large machines, especially those with significant power requirements, contribute to voltage sag, creating challenges for sensitive equipment.

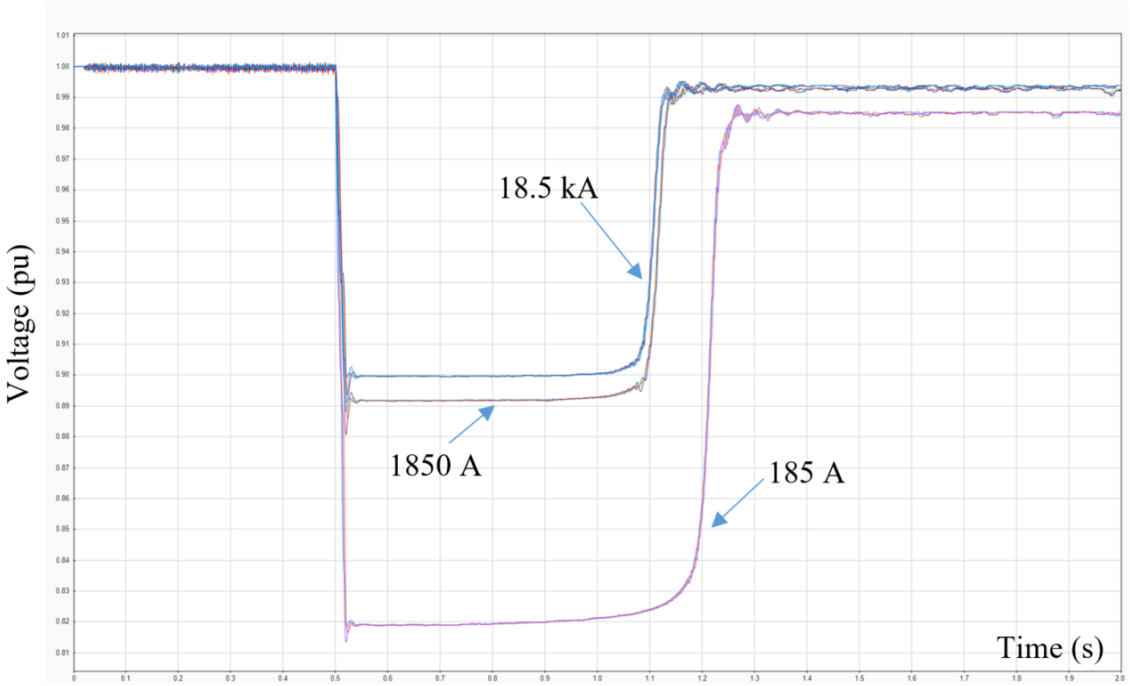


Figure 1-3 Voltage sag change with PCC fault level

Weak grids, which are inherently susceptible to voltage sag, face exacerbated issues in maintaining a steady voltage level due to the operation of large machines. The interaction between the machine operations and protective devices may lead to undesired tripping, affecting the overall reliability of the grid.

Figure 1-3 illustrates the impact of a large machine starting event on the system voltage at the PCC. The plot depicts voltage sags for various fault levels at the PCC. The severity of the voltage sags increases with decreasing grid strength, as evidenced by lower fault currents. Notably, the fault currents in this analysis are specified at the medium voltage level of 11 kV.

### 1.1.5 Simultaneous Operation of Machines

The simultaneous operation of machines can exacerbate voltage sag in a weak grid. When multiple machines or loads start operating simultaneously the combined effects, may lead to voltage sags. Therefore, it is necessary to implement mitigation strategies to ensure the reliable and uninterrupted operation of the system.

## Problem Statement

In the dynamic landscape of power systems, the integration of IBRs has become increasingly dominant. However, when dealing with weak distribution systems,

challenges can arise requiring the capability of IBRs to remain connected during the low voltage ride through.

Unbalanced voltage sag, in particular, poses a significant risk as it may lead to the disconnection of IBRs, introducing further complications in the power system.

Unbalanced voltage sag leads to disconnecting inverters from the grid, indicating a "G_PHASE" error [5].

Voltage sags can degrade the performance of induction motors within the system. A reduction in terminal voltage during a sag event directly affect to a decrease in motor torque [2].

Voltage sag can be caused due to simultaneous acceleration of motors or large machine operation. This, in turn, can disrupt the normal functioning of the system, emphasizing the importance of proactively addressing the issue of voltage sag in weak distribution systems [2].

## Scope

This research aims to provide insights into the effectiveness of these mitigation strategies in enhancing the resilience of weak distribution systems against voltage sag. The study is focused on examining voltage sag phenomena in a distribution system with lower fault levels with higher concentrations of IBRs. The proposed sag mitigation approaches include the implementation of a load management scheme and the robust operation of inverters. The load management scheme is designed based on a predetermined order of priority and considers the unique characteristics of loads within the system.

This thesis is bounded on addressing voltage sag mitigation, but will not cover the areas related to steady state stability. To cover such an approach, it should include the examination of parameters like system damping, eigenvalue analysis, and the impact of reactive power compensation. It would contribute to a holistic analysis of the distribution system's resilience.

## Objectives

The core objective of this research is to design a hybrid voltage sag mitigation technique for a renewable integrated weak distribution system, by designing a load

management algorithm, and a robust inverter control system that can remain connected to the system during events of voltage sag.

The research will focus on two specific objectives to achieve this goal:

- Designing of an algorithm for implementing a pre-assigned priority load management scheme to mitigate voltage sag.
- Designing of a robust inverter control system that can remain connected to the system during events of voltage sag.

# CHAPTER 2

# LITERATURE REVIEW

## Conventional Phase Locked Loop

The most widely used technique for achieving frequency independent grid synchronization in three-phase systems is the Synchronous Reference Frame-Phase Locked Loop (SRF-PLL). The conventional SRF-PLL employs Park's transformation to convert the three-phase voltage vector from the stationary reference frame to the synchronous reference frame. The angular position of this synchronous reference frame is regulated by a feedback loop, ensuring the q component transforms to zero.

In SRF-PLL, the transformation to the synchronous reference frame has been rescaled by a 2/3 factor. This scaling specifically allows the system to directly measure the amplitude of the incoming sinusoidal voltage signal [6], [7].

During normal operation conditions, the d component directly reflects the amplitude of the positive sequence sinusoidal input voltage ($V^{+1}$). Its phase angle is determined by the feedback loop output.

Under ideal grid conditions, free from harmonics and voltage unbalances, a wide bandwidth for the SRF-PLL feedback loop enables rapid and precise determination of the grid voltage's phase angle and amplitude. The SRF-PLL detects the amplitude and phase angle of the balanced input voltage vector by setting the q-axis component of the dq reference frame voltage ($v_q$) equal to zero, $v_q = 0$. [8], [9].

By strategically selecting a narrow bandwidth for the PLL, the response is enhanced by reducing the impact of undesired signal components on the PLL output [6]. The control loop's bandwidth is configured to ensure $v_q$ is approximately 0. This adjustment enables the PLL to promptly follow the variations in the balanced voltage vector applied at its input.

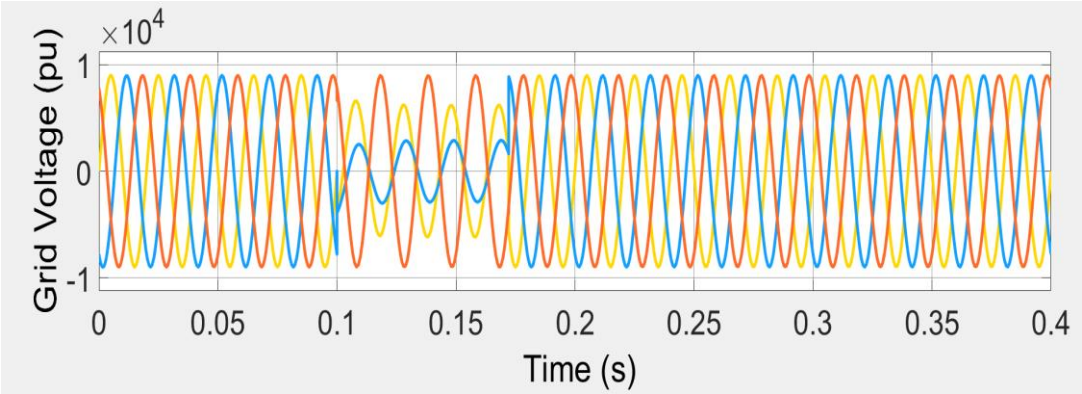


Figure 2-1 Unbalanced Voltage

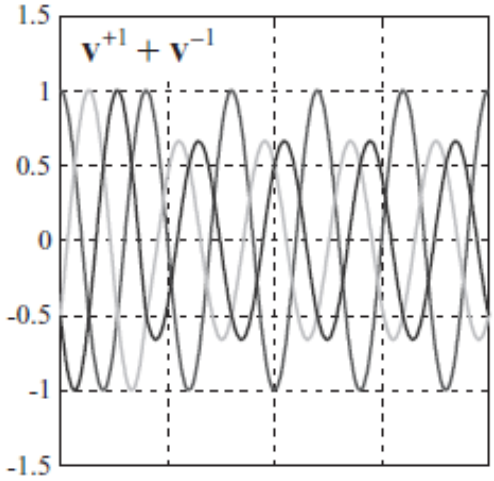


Figure 2-2 Sequence components of unbalanced voltage [8]

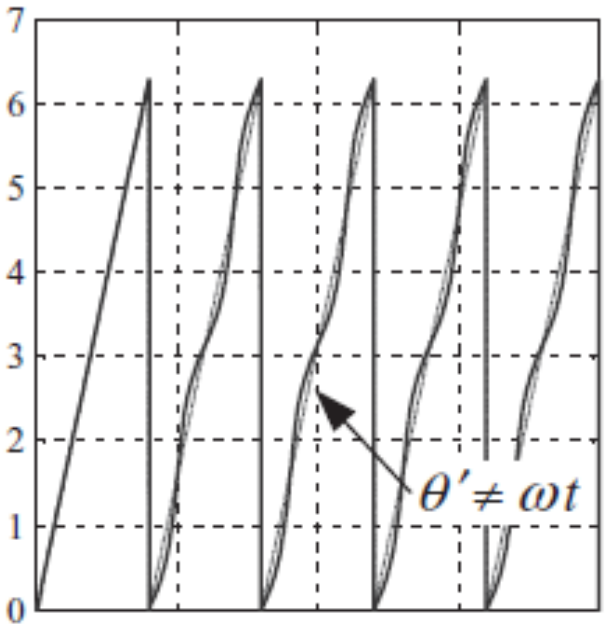


Figure 2-3 Phase angle during the unbalanced period [8].

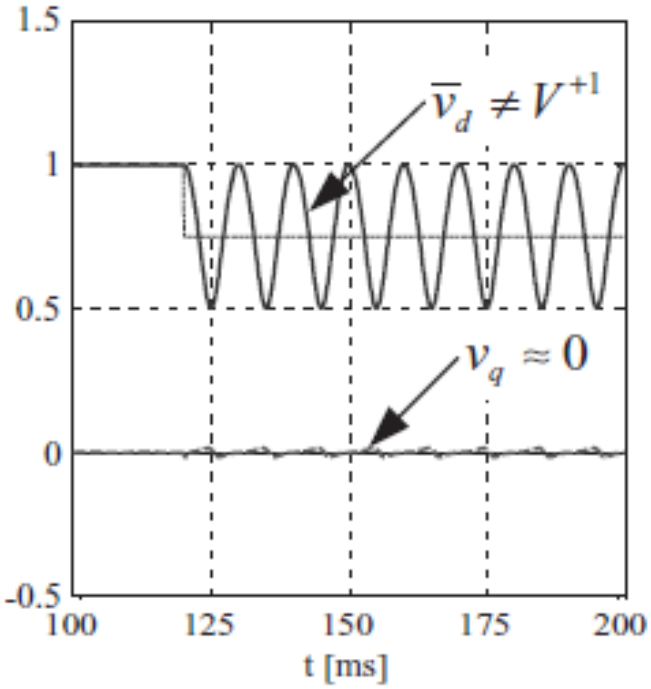


Figure 2-4 Oscillatory signal generates for the $v_d$ component using SRF-PLL. [8]

Conventional filtering techniques alone are insufficient for accurately evaluating the positive sequence component by extracting the average value of the d-axis component of the synchronous reference frame voltage ($v_d$) [8], [9].

Figure 2-1 indicates the unbalanced voltage sag in a grid while corresponding positive and negative sequence component representations are presented in Figure 2-2. Figure 2-3 presents the measured phase angle using SRF-PLL. The SRF-PLL cannot segregate the positive sequence component during an unbalanced voltage sag event. This is because the oscillatory $v_d$ component does not directly provide information related to the positive sequence component. Instead, it represents a combination of both positive and negative sequence components. This limitation is illustrated in Figure 2-4.

## Conventional Inverter Control System Drawbacks

The design of grid-connected power converters necessitates careful consideration to ensure their functionality under diverse grid voltage conditions. Developing robust and secure control algorithms is paramount, particularly when the grid experiences abnormal events. Grid faults are a prevalent source of such abnormalities, some

leading to unbalanced grid voltages at the converter's PCC. Consequently, the injected currents deviate from their typical balanced and sinusoidal waveforms.

Unbalanced grid voltages, often resulting from grid faults, introduce distorted currents into the power converter's output. The interaction between these distorted currents and the unbalanced voltages can lead to uncontrolled oscillations in the active and reactive power delivered to the grid. This scenario presents a significant control challenge, as many conventional current control algorithms employed in the industry exhibit limitations in accurately regulating the injection of unbalanced currents.

The effectiveness of a power converter's interaction with the grid under fault conditions hinges on the control strategy employed for generating reference currents. This process of reference current generation during grid faults is a critical aspect of power converter control. The selection of these current set points directly influences the converter's overall performance and its ability to deliver a specified amount of active and reactive power [8], [9], [10].

Maintaining control over the currents injected by the power converter into the grid phases is crucial, especially during significant grid voltage variations. To achieve this, the control algorithms responsible for generating reference currents require continuous estimation of the instantaneous behavior of these phase currents. Accurate real-time estimation, including during transient fault conditions, is essential to prevent overcurrent tripping events.

According to IEEE 1547-2018, three-phase Distribution Energy Resources may cease to energize and trip if the negative sequence component of the applicable voltage is greater than 5% of the nominal voltage for greater than 60 s or greater than 3% of the nominal voltage for greater than 300 s, provided that the voltage unbalance is neither caused nor aggravated by unbalanced currents of the local electric power system [11]. The inability to achieve accurate control during unbalance may result in damage to the inverter. Therefore, as a preventive measure, this standard limit the LVRT capability during an unbalanced event. From a power system perspective, the unavailability of generation during such grid disturbances can lead to significant issues.

## Decoupled Double Synchronous Reference Frame -Phase Locked Loop (DDSRF-PLL)

By employing this DDSRF approach, the positive sequence voltage component and negative sequence component can be decoupled separately. This is accomplished by defining two distinct reference frames of dq synchronous reference. This capability facilitates precise grid synchronization, even in the presence of unbalanced voltages [8].

This reference frame comprises two orthogonal rotating axes: a positive-sequence frame ($dq^+$) rotating in the positive direction with an angular position of $\theta^+$, and a negative-sequence frame ($dq^-$) rotating in the negative direction with an angular position of $\theta^-$.

$$V_{dq^+} = \begin{vmatrix} V_{d^+} \\ V_{q^+} \end{vmatrix} = [T_{dq^+}].V_{\alpha\beta} \quad (2\text{-}1)$$

$$V_{dq^-} = \begin{vmatrix} V_{d^-} \\ V_{q^-} \end{vmatrix} = [T_{dq^-}].V_{\alpha\beta} \quad (2\text{-}2)$$

$$[T_{dq^+}] = [T_{dq^-}]^T = \begin{vmatrix} \cos(\theta) & sin(\theta) \\ -\sin(\theta) & \cos(\theta) \end{vmatrix} \quad (2\text{-}3)$$

Equation (2-1) shows the transform equation of the positive sequence dq components utilizing alpha-beta coordinates, with the transformation matrix presented in (2-3). Similarly, (2-2) outlines the equation for the negative sequence dq components [8], [9], [10].

The DC values of the $dq^+$ and $dq^-$ frames correspond to the amplitude of the sinusoidal signals $v^+$ and $v^-$, respectively, and the coupling between these leads to oscillations at $2\omega$. This coupling effect can be eliminated by considering the decoupling of oscillatory components [8].

There are some other methods also available for achieving accurate grid synchronization in power converter controllers, which can be implemented using a stationary reference frame. One of the methods involves the use of resonant controllers. In resonant controllers, the grid frequency is utilized for grid

synchronization. However, with the DDSRF-PLL, instead of using the grid frequency, grid voltage phase angle is used as the synchronization variable [8], [9], [10].

## Flexible Positive and Negative Sequence Control (FPNSC)

There are several methods available for injecting current during grid voltage unbalanced conditions, and for this research, the Flexible Positive and Negative Sequence Control (FPNSC) method [19] is employed.

Taking into account various limitations like power oscillations and the capabilities of active, reactive power injection with the mentioned strategies, FPNSC is emerging as a better method for generating reference currents via power converters, especially in scenarios involving unbalanced grid conditions.

The equation for deriving the active reference current vector ($i_p^*$) is obtained by decoupling the instantaneous conductance by the positive sequence conductance ($G^+$) and negative sequence conductance ($G^-$). The derived equation for the active reference current vector is showed by (2-4).

$$i_p^* = G^+V^+ + G^-V^- \quad (2\text{-}4)$$

The active power current also includes a negative sequence component, allowing the injection of either positive or negative sequence currents into the grid based on the grid condition.

However, for precise delivery of a desired active power (P) to the grid, controlling the injected current necessitates simultaneous control of both positive and negative sequence components. This is due to their combined influence on the total active power injection. To achieve this dual control, a scalar parameter (k1) is introduced to regulate the contribution of each sequence component to the reference active power currents.

$$i_p^* = k_1 \frac{P}{|v^+|^2} v^+ + (1 - k_1) \frac{P}{|v^-|^2} v^- \quad (2\text{-}5)$$

A similar concept can be applied for deriving the reactive current, wherein the scalar parameter is named as $k_2$. By utilizing this parameter, the given amount of reactive

power injection to the grid can be controlled. The respective equations with the scalars are shown in (2-5) and (2-6).

$$i_q^* = k_2 \frac{Q}{|v^+|^2} v^+{}_\perp + (1 - k_2) \frac{Q}{|v^-|^2} v^-{}_\perp \quad (2\text{-}6)$$

An equation for the total current injection by the inverter can be formulated utilizing these relationships. The respective equation with the scalars are shown in (2-7), control over the positive and negative sequence components of active power and reactive power is achieved by adjusting $k_1$ and $k_2$. This flexibility allows us to deliver current based on grid measurements, effectively mitigating voltage sag [20], [21].

$$i^* = P\left[k_1 \frac{1}{|v^+|^2} v^+ + (1 - k_1) \frac{1}{|v^-|^2} v^-\right] + Q\left[k_2 \frac{1}{|v^+|^2} v^+{}_\perp + (1 - k_2) \frac{1}{|v^-|^2} v^-{}_\perp\right] \quad (2\text{-}7)$$

## Inverter Controller during Voltage Sag

The integration of Inverter-Based Resources (IBRs) into power grids necessitates robust control strategies for seamless operation under diverse grid conditions. These strategies address two critical objectives: preventing unnecessary tripping of the converter's protection system and supporting the grid voltage during Low Voltage Ride Through (LVRT) conditions.

Unbalanced faults on the grid typically introduce negative sequence components into the voltage waveforms at the IBR's connection point. Under these unbalanced conditions, the currents injected by the inverter deviate from their ideal sinusoidal and balanced patterns. This interaction between the unbalanced grid voltages and the injected currents can lead to uncontrolled oscillations in both the active and reactive power delivered by the IBR, further exacerbating grid instability. [20], [21].

## Estimation of Over Current Limits

Due to the injection of unbalanced currents into the grid by FPNSC method, the instantaneous current may differ from phase to phase. Therefore, accurate current control is needed to prevent undesired tripping of the inverter. However, the locus of the operating current of the inverter is changed based on the selected operating strategy during unbalanced conditions. Additionally, factors considered under the strategy,

such as active power oscillation, active reactive power oscillation, or harmonic current injection, lead to changes in the corresponding equations.

At any given moment, the total current injected by the inverter should equal the sum of the active current ($i_p^*$) and the reactive current ($i_q^*$). Adjusting the values of $k_1$ and $k_2$ allows for the injection of a specific amount of active and reactive power. By deriving an equation for total current based on the set point of total current injection, can establish the locus of the operating current.

To define a current vector, the instantaneous values of its alpha-beta reference frame need to be defined. Equation (2-8) presents the mathematical representation of $i_p^*$ current vector, where $I_{pL}$ and $I_{pS}$ denote the modulus of two rotating vectors. $I_{pL}$ corresponds to the value of the large axis of the $i_p^*$ ellipse, while $I_{pS}$ represents the magnitude of its short axis. Equation (2-9) provides the same representation for $i_q^*$ [22].

$$i_p^* = \begin{bmatrix} i_{p\alpha}^* \\ i_{p\beta}^* \end{bmatrix} = \begin{bmatrix} I_{pL} cos\omega t \\ I_{pS} sin\omega t \end{bmatrix} \quad (2\text{-}8)$$

$$i_q^* = \begin{bmatrix} i_{q\alpha}^* \\ i_{q\beta}^* \end{bmatrix} = \begin{bmatrix} -I_{qS} sin\omega t \\ I_{qL} cos\omega t \end{bmatrix} \quad (2\text{-}9)$$

With these overcurrent limits, the maximum current in each phase can be estimated. The derived equation for power injection using the inverter can be formulated, as shown in (2-10). Depending on the mode of operation, both active power and reactive power, as well as the maximum reactive power, can be delivered to the grid.

The value of γ differs depending on the phase, whether it is a, b, or c. Generally, for phase a, γ is equal to δ, where δ represents the angle difference between a phase and the $i_p^*$ [22].

$$\begin{aligned} I^2 = {} & P^2 \left[ \frac{k_1^2 . |v^-|^2 + (1-k_1)^2 . |v^+|^2 + 2k_1(1-k_1) cos2\gamma . |v^+| . |v^-|}{|v^+|^2 . |v^-|^2} \right] \\ & + Q^2 \left[ \frac{k_2^2 . |v^-|^2 + (1-k_2)^2 . |v^+|^2 + 2k_2(1-k_2) cos2\gamma . |v^+| . |v^-|}{|v^+|^2 . |v^-|^2} \right] \\ & - PQ \left[ \frac{(2k_1 + 2k_2 - 4k_1k_2)|v^+| . |v^-| . sin2\gamma}{|v^+|^2 . |v^-|^2} \right] \end{aligned} \quad (2\text{-}10)$$

## Removal of Coupling Effects in DDSRF-PLL

The decoupled reference frames in DDSRF voltage vectors are rotated with $+\omega$ and $-\omega$ frequencies respectively. The $v_{dq}^{+}$ and $v_{dq}^{-}$ can be represented as (2-11) and (2-12) respectively. It can be observed that these components consist of dc terms and ac terms.

For example, if oscillation generated by the voltage vector $v^{-}$ on the $dq^{+}$ axes signals needs to be cancelled out, $v^{-}$ signals can be utilized, and vice versa [23].

$$V_{dq^+} = \begin{vmatrix} V_{d^+} \\ V_{q^+} \end{vmatrix} = V^{+}\begin{bmatrix} cos(\varphi^{+1}) \\ sin(\varphi^{+1}) \end{bmatrix} + V^{-}cos(\varphi^{-})\begin{bmatrix} cos(2\omega t) \\ -sin(2\omega t) \end{bmatrix} + V^{-}sin(\varphi^{-})\begin{bmatrix} sin(2\omega t) \\ cos(2\omega t) \end{bmatrix} \quad (2\text{-}11)$$

$$V_{dq^-} = \begin{vmatrix} V_{d^-} \\ V_{q^-} \end{vmatrix} = V^{-}\begin{bmatrix} \cos(\varphi^{+1}) \\ \sin(\varphi^{+1}) \end{bmatrix} + V^{+}\cos(\varphi^{+})\begin{bmatrix} \cos(2\omega t) \\ \sin(2\omega t) \end{bmatrix} + V^{+}\sin(\varphi^{+})\begin{bmatrix} -\sin(2\omega t) \\ \cos(2\omega t) \end{bmatrix} \quad (2\text{-}12)$$

Furthermore, in (2-4), the $V^{+}\begin{bmatrix} \cos(\varphi^{+}) \\ \sin(\varphi^{+}) \end{bmatrix}$ term represents the DC component, while the $V^{-}\cos(\varphi^{-})\begin{bmatrix} \cos(2\omega t) \\ -\sin(2\omega t) \end{bmatrix} + V^{-}\sin(\varphi^{-})\begin{bmatrix} \sin(2\omega t) \\ \cos(2\omega t) \end{bmatrix}$ term represents the AC component [23].

## Loads Behaviour during Voltage Sag

Computers, consumer electronics, and certain process control equipment commonly employ single-phase diode rectifiers to convert AC power to DC. However, during voltage sag, tripping often occurs, primarily due to under-voltage protection activating because of a reduction in DC bus or AC incoming voltage.

Adjustable speed AC drives (ASD) typically receive power through a three-phase rectifier and are sensitive to voltage sag. Shallow and short sags might cause minor issues like reduced torque, while deep and prolonged ones can lead to tripping. Different ASD control strategies have varying degrees of tolerance while firing-angle control (FAC) drives may experience phase-angle jumps, other control methods can also be affected, leading to diverse issues like increased distortion, reduced torque, or instability [2], [14]. Tripping can occur due to various phenomena:

- The motor drive controller's protection system detects sudden changes in operating conditions, triggering tripping mechanisms to prevent damage to power electronic components.

- The voltage drop in the DC bus during the sag could lead to malfunctions or trigger the tripping of the motor drive controller.
- Voltage sags can result in increased AC currents within ASDs. This overload can activate overcurrent protection measures such as trips or blown fuses, safeguarding the power electronics.

Voltage sag directly affects the operation of induction motors. The basis of induction motor operation lies in the generation of magnetic flux within the motor. The motor's torque production is directly proportional to the product of voltage and current. In Figure 2-5, the magnetic flux of a 5.5 kW motor is shown during normal operation under 85% rated loading.

When a voltage sag occurs, the reduced voltage directly impacts the magnetic flux levels in the motor, resulting in a reduction in the motor's torque production capability.

The duration of the voltage sag is a crucial factor in determining the severity of its impact on the induction motor. Prolonged voltage sags can have more severe consequences, potentially leading to damage and long-term operational issues. In Figure 2-6, the magnetic flux reduction due to a 30% voltage sag is shown [15], [16].

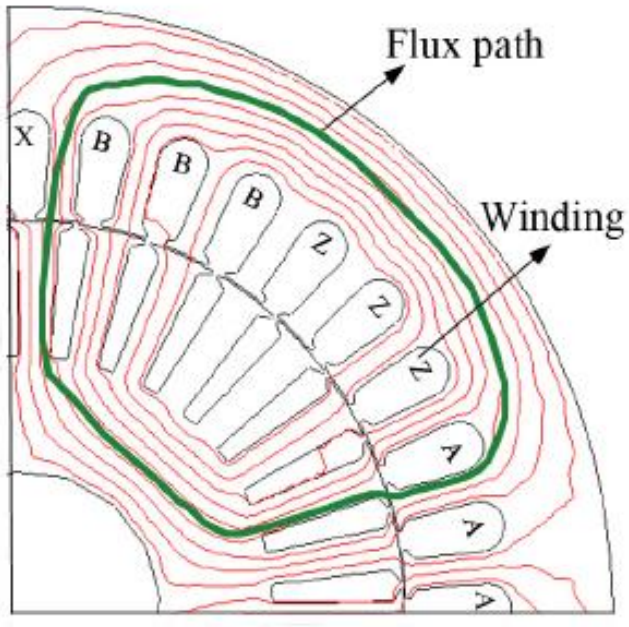


Figure 2-5 The magnetic flux of 5.5 kW induction motor with 85% rated load. The magnetic flux of normal operation [16]

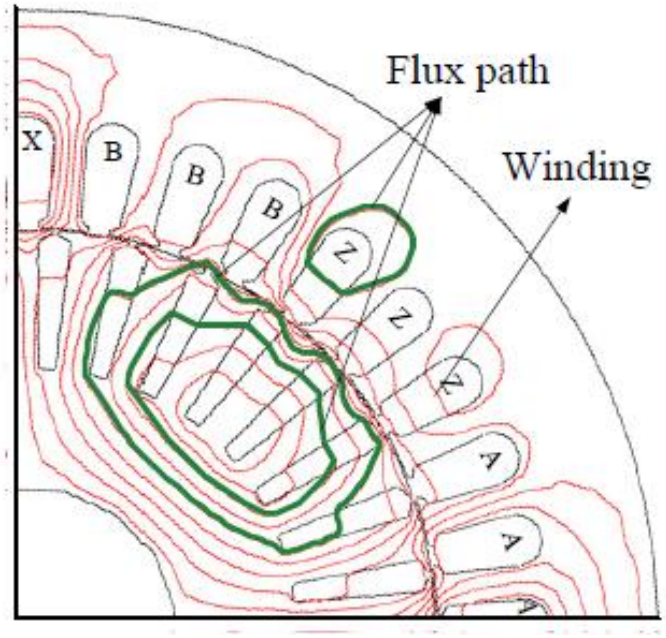


Figure 2-6 The magnetic flux at half cycle since the 30% voltage sag [16].

Once the voltage is restored to its rated level, the induction motor initiates a recovery process to restore its flux. During this phase, the motor strives to return to its normal operating conditions. As the voltage returns to its regular level, the magnetic flux levels in the motor increase, allowing the motor to regain its ability to generate the required torque for optimal performance while experiencing higher inrush current [16].

## Equipment Sensitivity for Voltage Sag

Electrical equipment is often sensitive to voltage sags, leading to variations in performance and output depending on the severity of the sag. Power electronics-based equipment, such as workstations, servers, and PLCs, are particularly vulnerable to voltage sags. To address the behaviour of these sensitive devices, various standards define acceptable durations for voltage sags.

Some common effects of voltage sags on computer equipment include:

- Network servers may lose data due to voltage sags, especially Hard Disk Drive (HDD) storage systems.
- Voltage sags can cause operating system crashes, leading to server restarts. This can result in delays in workstation processes, particularly in industrial environments.

- Prolonged or frequent voltage sags may damage this sensitive power electronic equipment.

The CBEMA recognized the significance of voltage sag susceptibility in electronic equipment and introduced the CBEMA curve. This curve represents allowable voltage variations over time that sensitive electronic equipment can withstand without malfunctioning or experiencing damage. The CBEMA curve is essentially a guideline helping manufacturers and users understand the voltage tolerance limits of computer equipment [1].

It typically shows that electronic equipment can withstand short-duration voltage sags without adverse effects. However, as the duration increases, the allowable voltage deviation decreases. Beyond certain limits, prolonged or severe voltage sags can lead to data loss, equipment malfunctions, and, in extreme cases, permanent damage.

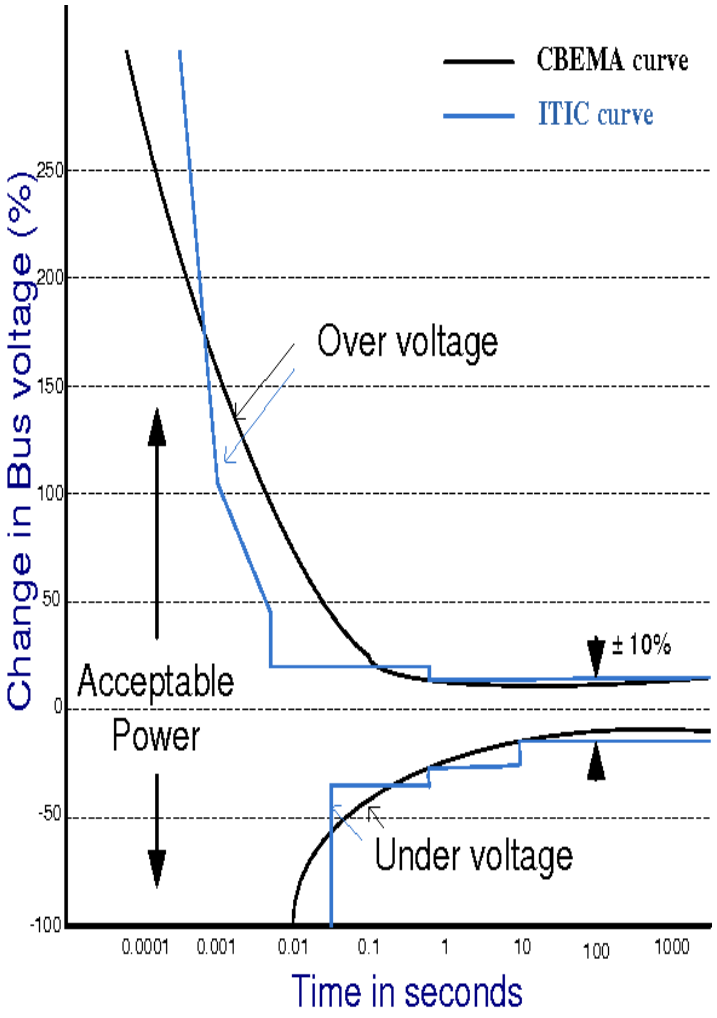


Figure 2-7 Old CBEMA and ITIC curves [17]

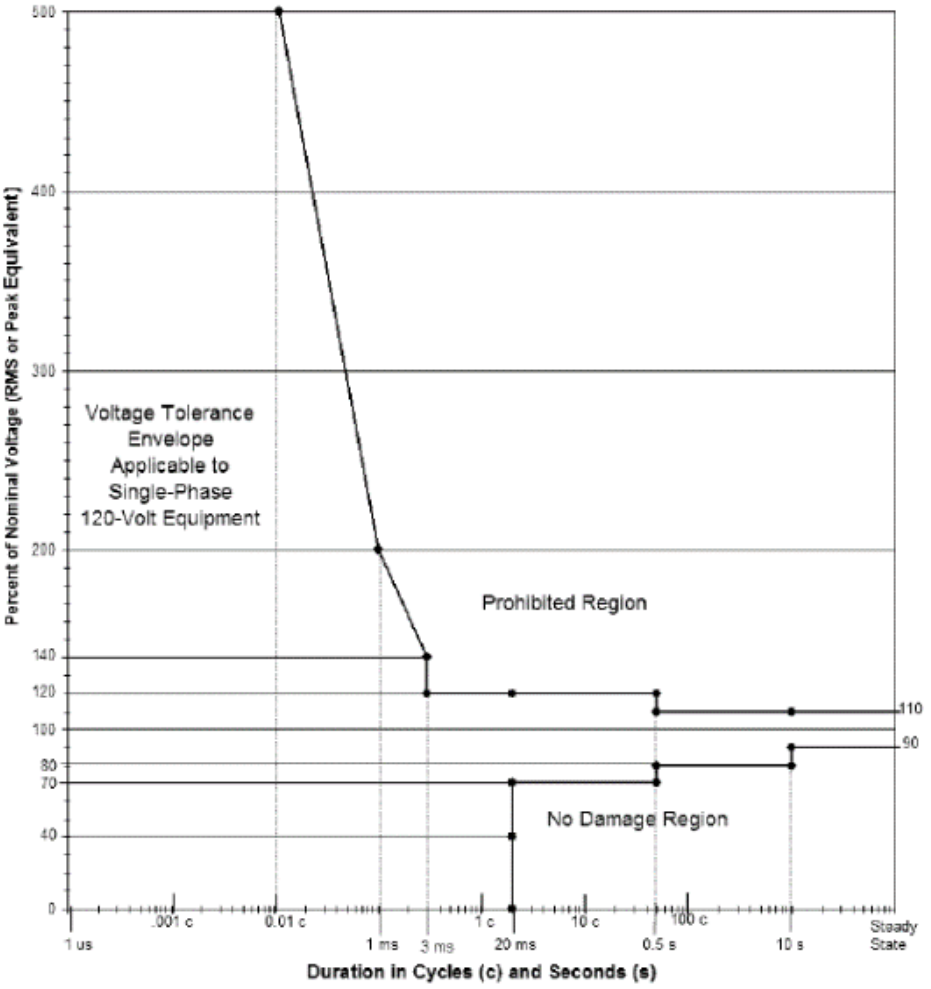


Figure 2-8 New ITI (CBEMA) curve (2000) [18]

Various associations define their own susceptibility curves for voltage sag. Figure 2-7 shows the old CBEMA and ITIC curves. However, the ANSI standardized the CBEMA curve in ANSI/IEEE 1100 standard. Figure 2-8 shows the New ITI (CBEMA) curve used in the IEEE 1100 standard [18].

# CHAPTER 3

# METHODOLOGY

## General Illustration

In this chapter, a brief overview of the implemented system is provided. The system consists of two main subsystems:

1. operation of the inverter under unbalanced conditions
2. load management for voltage sag mitigation

***Operation of the inverter under unbalanced conditions***

A simplified overview of the proposed subsystem for the inverter control is illustrated in Figure 3-1. Under normal grid operating conditions, the inverter is operated in a predetermined mode. For example, if used as a solar inverter, maximum power point tracking mode can be employed. When voltage unbalance occurs, it is detected by the inverter's control system. Based on the unbalanced voltage, the inverter switches from its current operating mode to the proposed mode of mitigating unbalanced voltage sag.

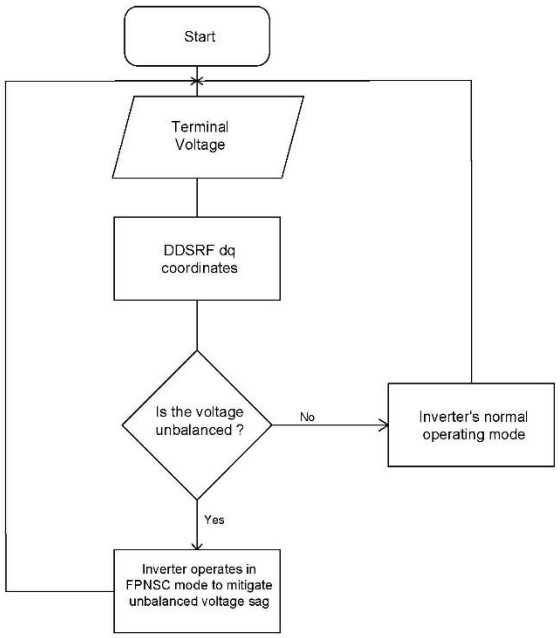


Figure 3-1 Flowchart of Inverter operation mode to mitigate unbalanced voltage sag

Once the voltage is restored, it reverts back to the normal operation. The proposed control mode enables the inverter to remain connected during unbalanced voltage sag and supports grid stability.

***Load management for voltage sag mitigation***

The second subsystem is the load management system. As elaborated in previous sections, in weak grids, large machine operations often result in significant voltage sags, which varies depending on the load type. Thereby, this subsystem was developed to successfully integrate these large loads into the system and prevent voltage sag violations.

It systematically connects loads while monitoring voltage sag levels. Figure 3-2 shows the flowchart of the simplified system, illustrating the process. It first categorize the voltage sag based on predefined severity levels. Depending on the severity level, the load shedding scheme is activated upon voltage sag identification to restore the voltage back to normal levels.

The load shedding scheme operates based on each load's priority level. Once the voltage is successfully restored, the voltage sag detection system allows the system to gradually reconnect all disconnected loads, thereby enabling the system to fully restore all the loads those were shedded.

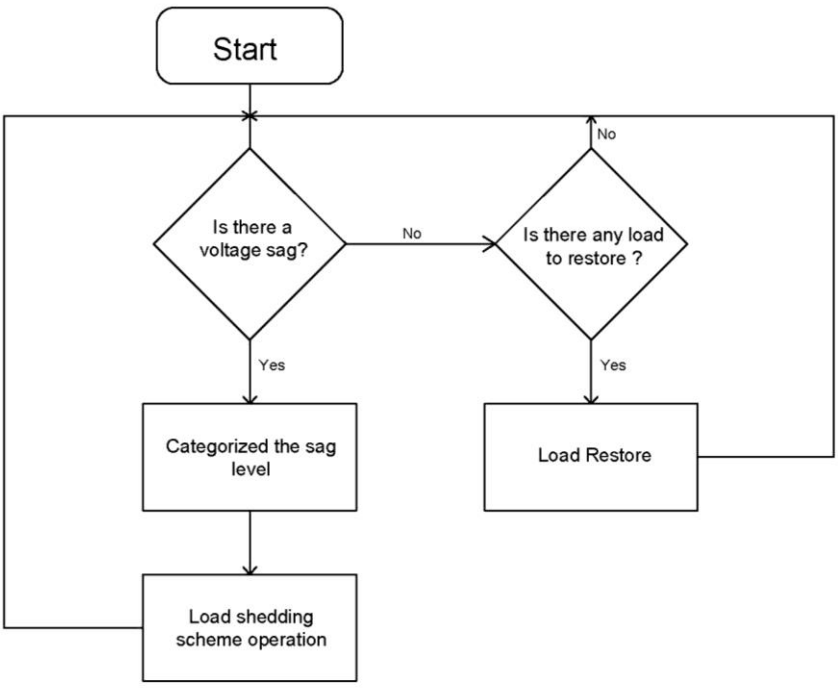


Figure 3-2 Flowchart of Load Management System

# CHAPTER 4

# MODELING APPROACH

## Inverter Unbalanced Operation

### 4.1.1 Decoupled Double Synchronous Reference Frame -Phase Locked Loop (DDSRF-PLL)

The DDSRF-PLL method is considered a better and more accurate synchronization technique during grid voltage unbalance for inverter control system. The system is modelled using MATLAB in order to simulate and demonstrate the performance during voltage sag. As mentioned in the Chapter 2, the coupling effect of the positive and negative sequence components introduces oscillatory components in the output signal.

Figure 4-1 shows the positive sequence oscillatory component before the removal of the coupling effect, while Figure 4-2 shows the negative sequence oscillatory signal prior to removing the coupling effect. After the signal is converted to the dq coordinate system, the unwanted coupling components need to be removed. Eliminating this coupling effect results in a usable signal for effective control.

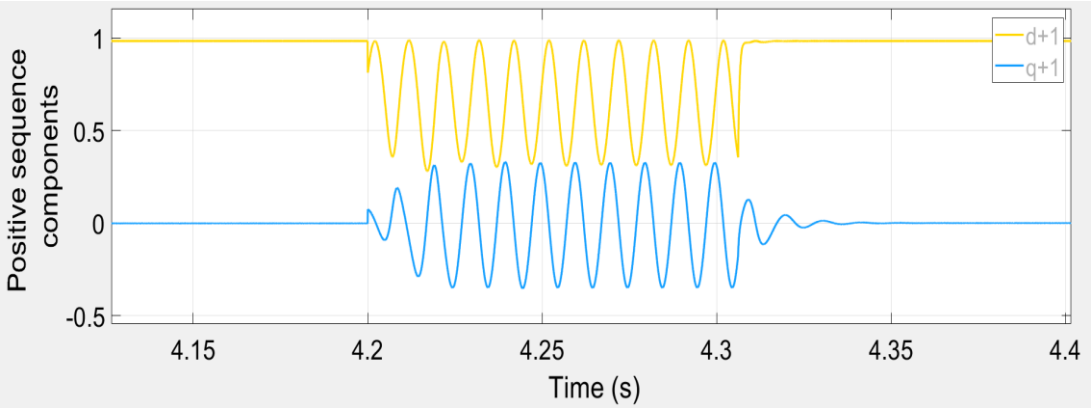


Figure 4-1 Positive sequence component during the unbalanced voltage sag

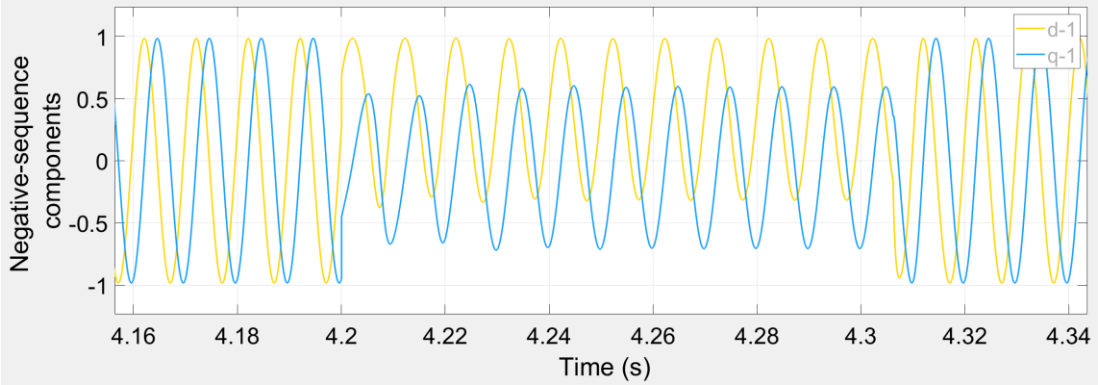


Figure 4-2 Negative sequence component during the unbalanced voltage sag

Figure 4-3 and Figure 4-4 respectively present the three-phase voltage and the detected phase angle using DDRF-PLL during a grid fault. It can be observed from Figure 4-3 that this grid fault results in voltage unbalance and voltage sag in the grid voltage.

During the process of segregating the positive- and negative-sequence dq components, cross-coupling between the d-axis and q-axis signals of both synchronous reference frames can arise. This phenomenon is further illustrated in Figures 4-5 and 4-6.

Figure 4-5 shows the positive-sequence dq components, providing a clearer understanding of the oscillatory component. It differentiates between the filtered d-axis component ($d^{+'}$) and the d-axis component with the coupling effect ($d^{+}$). The same applies to the q-axis component.

Figure 4-6 focuses on the negative-sequence dq components. Under normal balanced operation, there should be minimal to no negative sequence component present in the grid voltage.

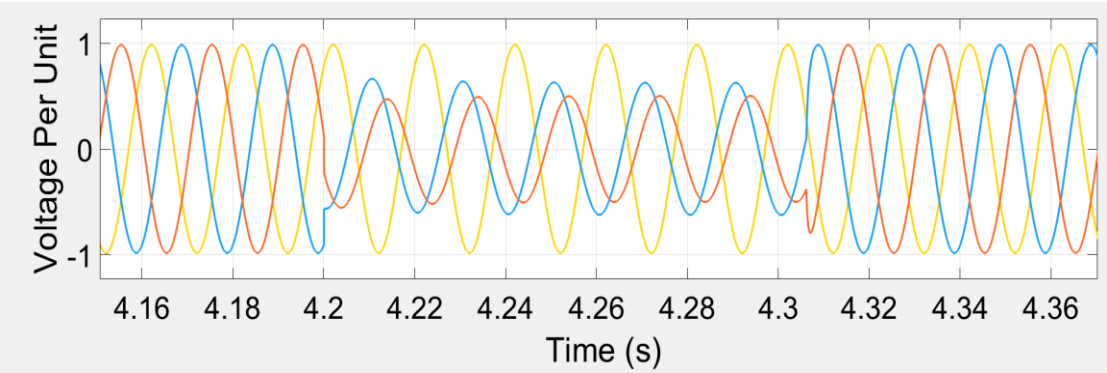


Figure 4-3 Grid voltages during unbalance

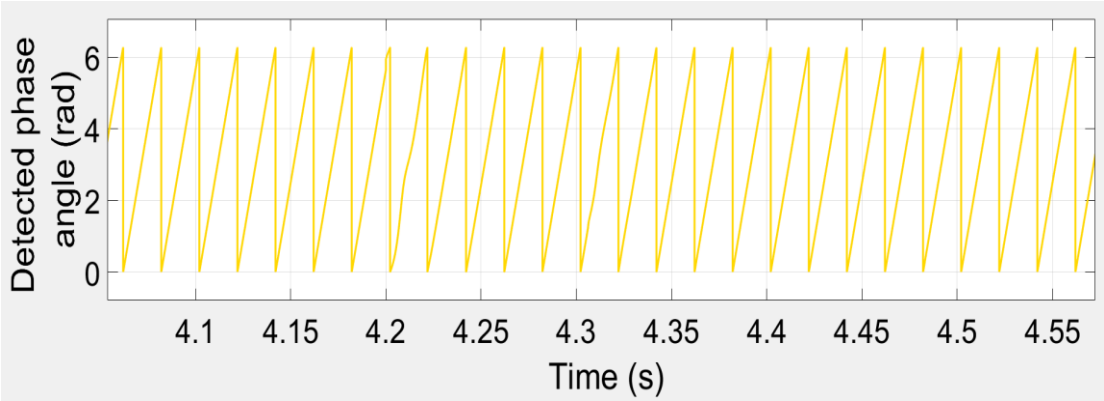


Figure 4-4 Phase angle during the unbalance

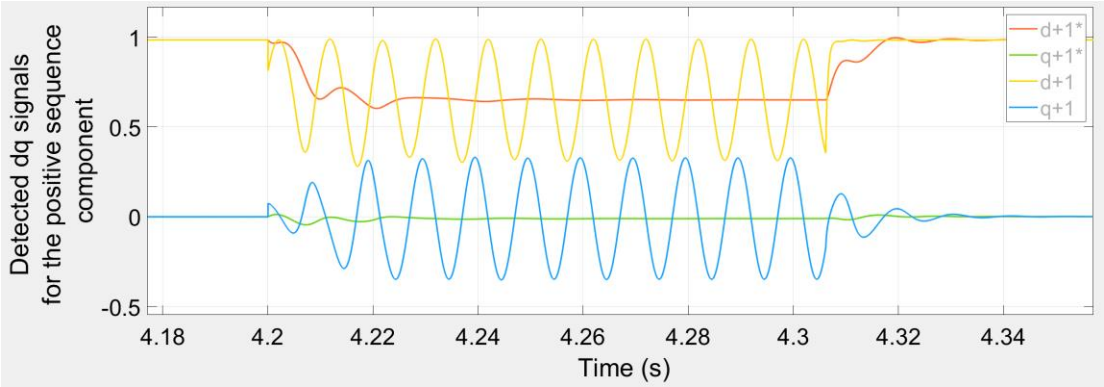


Figure 4-5 Detected dq signals for the positive sequence component

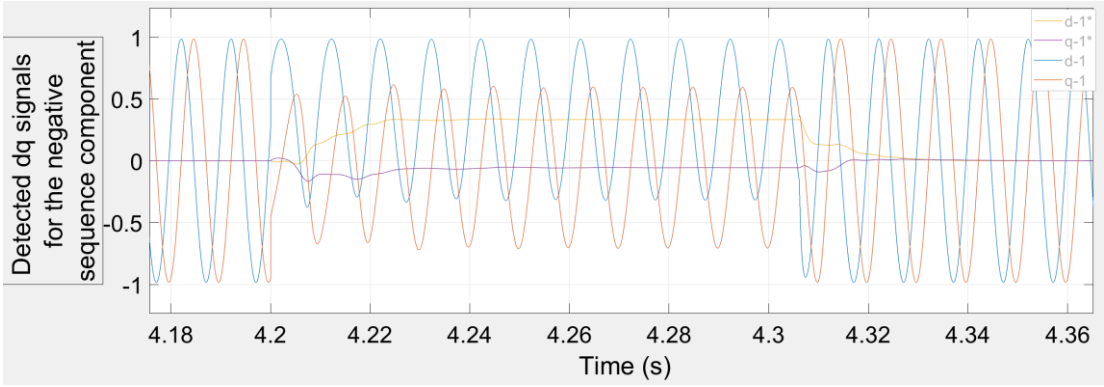


Figure 4-6 Detected dq signals for the negative sequence component

However, Figure 4-6 highlights that unbalanced faults can introduce a significant negative sequence component. A block diagram representation of the control model is provided in Figure 4-7. This diagram clarifies the signal flow and processing steps within the control system. The following functionalities are detailed in the block diagram:

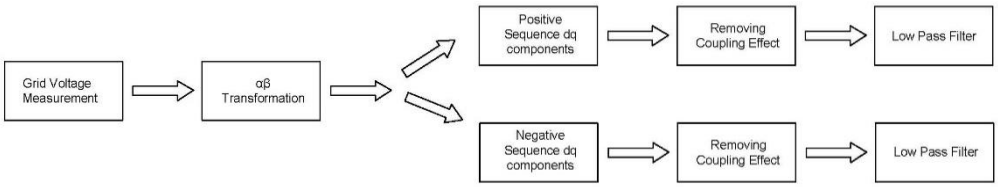


Figure 4-7 Block diagram of grid voltage decomposition

- Grid Voltage Measurement: This block represents the acquisition of grid voltage measurements (abc reference frame).
- αβ Transformation: This block demonstrates the conversion of abc reference frame voltages into the αβ coordinate system.
- Positive and Negative Sequence Decoupling: This block shows the separation of positive and negative sequence components using the transformation matrices discussed in (2-1) and (2-2), respectively.
- Low-Pass Filtering: This block represents the removal of high-frequency components from the processed signal to ensure accurate information is provided to the control system.

### 4.1.2 Flexible Positive and Negative Sequence Control (FPNSC)

The injection of currents during voltage unbalanced periods is enabled by the inverter control operation done by the FPNSC strategy, with the maximum peak value of the current serving as the operating limit. Based on this current limit set point, active and reactive injection as well as maximum reactive power injection are executed, aligning with the power injection requirements.

To avoid overcurrent limit violations in the inverter, the set point dynamically adjusts the output current, preventing overcurrent operation.

## Load Management System

### 4.1.3 Sag Detection for Load Management Scheme

To develop an accurate voltage sag detection system, a combined approach is employed, as shown in Figure 4-9, integrating both the rms voltage levels and the analysis of the rate of change of rms voltage.

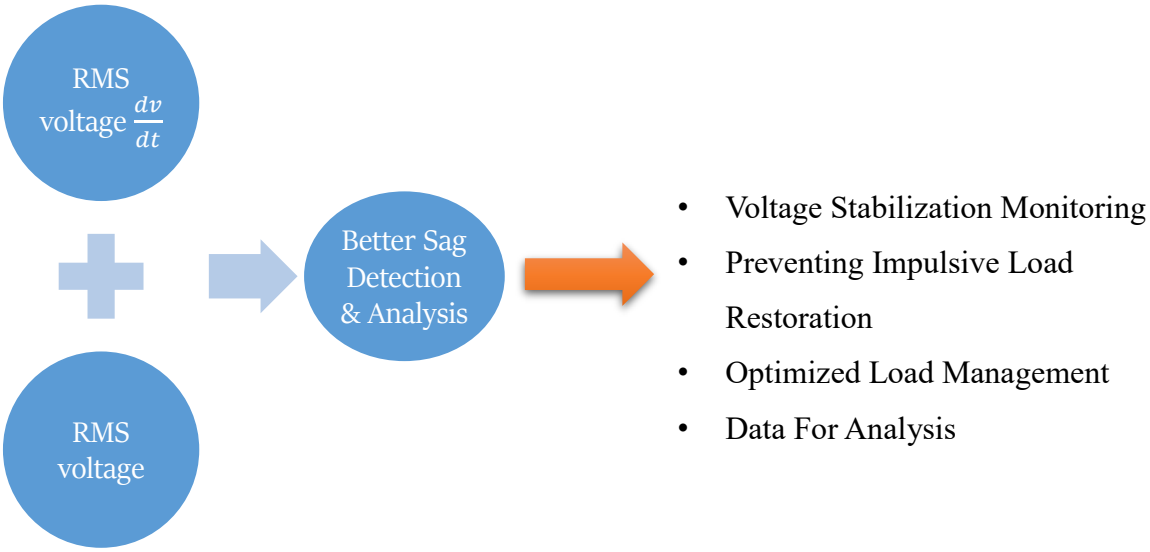


Figure 4-8 Load management scheme detection technique

This combined method ensures the accuracy of voltage sag detection, confirming the voltage is stable before proceeding to the next execution phase. The integration of the rms voltage sag level and its rate of change enables voltage stabilization monitoring. Additionally, this approach contributes to preventing impulsive load restoration, thereby safeguarding against potential disruptions.

This combined approach facilitates optimized load management, enabling all loads to connect to the system while effectively reducing power quality issues arising from voltage sag. Data acquired from this system can be stored on a server to identify opportunities for future system enhancements. By analyzing this data, can gain valuable insights into the system's performance. This includes identifying patterns of large consumer load operations.

### 4.1.4 Load Prioritization Scheme

A distribution system consists of various types of loads that cater to the diverse energy needs of consumers. These loads include lighting, heating, and many other diverse needs in houses, shops, malls, and theatres, among other places. To address the challenges of sag mitigation in a weak distribution system, a load management-based approach is developed.

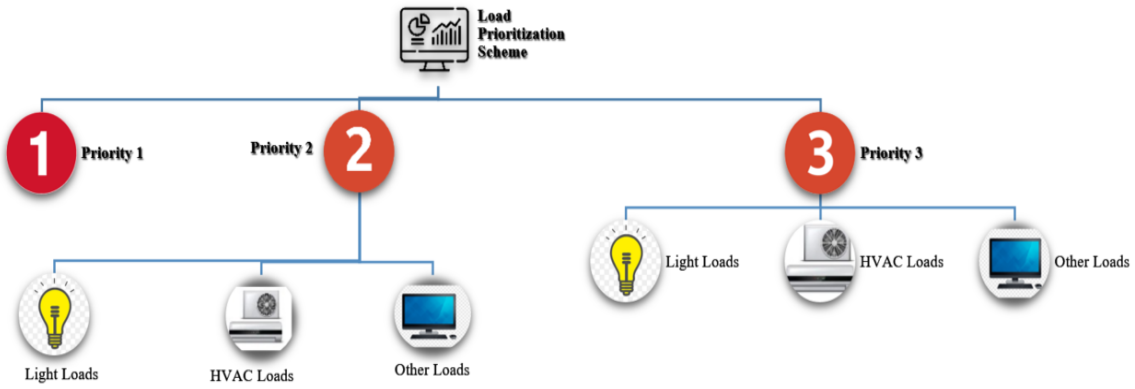


Figure 4-9 Load prioritization scheme

The core of the proposed scheme lies in a customer-defined load prioritization. Recognizing that different consumers have distinct energy requirements, this approach allows utilities to categorise interruptible loads based on individual needs. By incorporating this customer-centric approach, utilities can identify diverse consumer load priorities at different times of the day and implement this scheme with minimal disturbance for customer satisfaction.

As shown in Figure 4-10, the proposed scheme introduces three distinct levels of load priorities. Consumers can change their priorities based on the time of the day, ensuring that the loads are not interrupted with their requirement. Each load is assigned a priority level, with Level 1 being the highest and the subsequent levels descending in order.

To minimize the impact on customer satisfaction, load priority levels change based on the time of the day. Proposed time-dependent method considers off-peak times, peak times, and night time, and consumers can select their preference for the loads based on the time. This scheduling ensures catering to the dynamic requirements of consumers throughout the day.

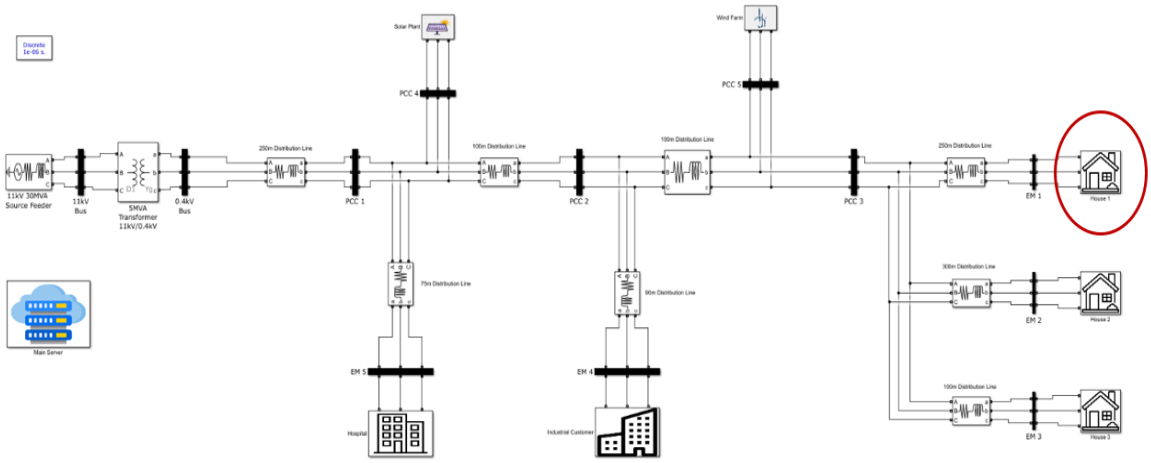

Figure 4-10 Implementation of proposed load management scheme

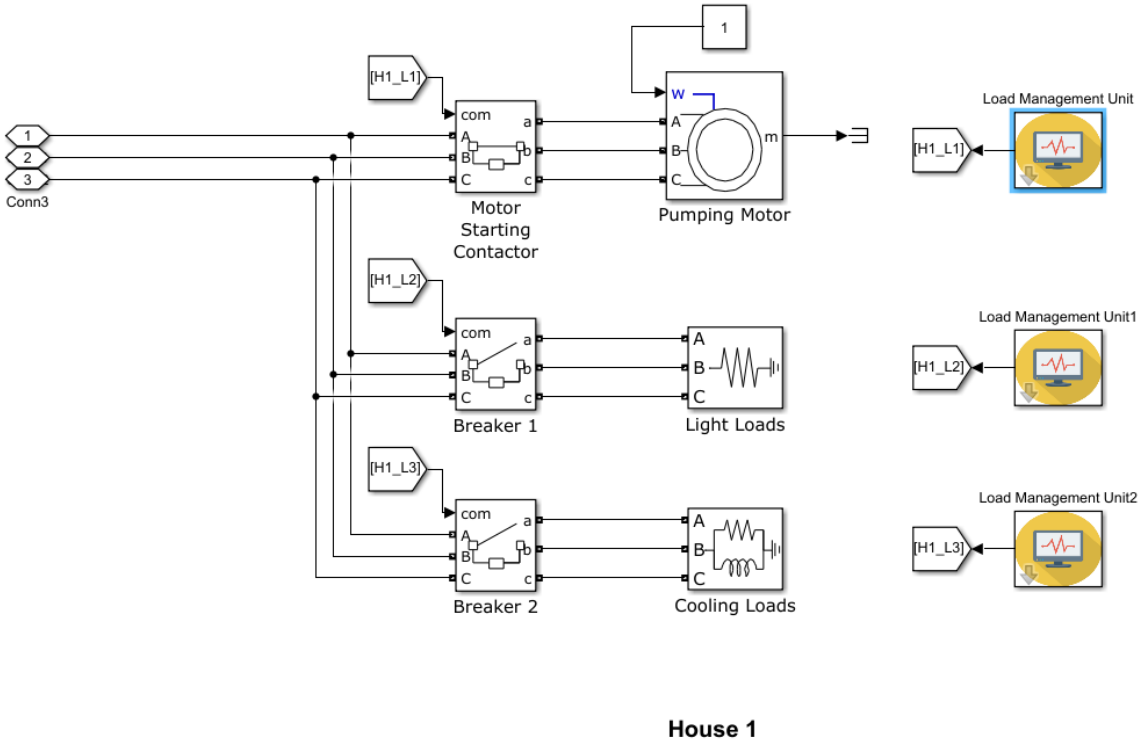


Figure 4-11 Implementation of proposed load management scheme

For example, as illustrated in Figure 4-11, in a small distribution network, each house or industry premises has a LMS system that enables customers to select their preferences. The first step involves customers selecting the load type, with three basic options: light, HVAC, and other. Subsequently, for each time period, the customer can choose the priority for the selected load.

The highest priority level is priority level 1. Loads categorized with Level 1 priority are not being shed during operation, irrespective of the system operation. This exclusivity ensures that critical or essential loads operate smoothly throughout the time period without any interruptions, thereby enhancing reliability and customer satisfaction. While priority 3 has the lowest priority, the load management scheme starts from this level. At any given moment, the central load management server has a record of the connected loads and their priorities, and this data is utilized to execute the scheme.

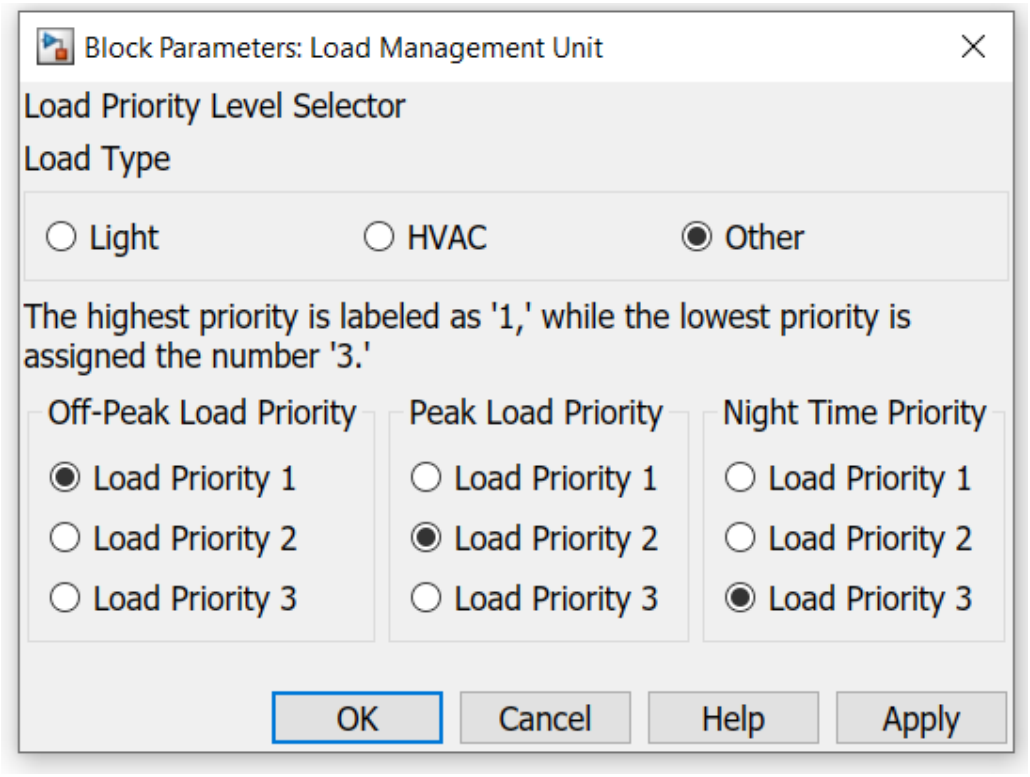


Figure 4-12 Load priority level selector interface

Figure 4-13 shows the load priority level selector interface available at each customer's premises. This system has the flexibility for the customer to define the priority level for their selected load. For example, if we consider implementing this selection for a ceiling fan, it would typically fall under the category of "other load." In this setup, during off-peak times, it is allocated the highest priority (level 1), during peak times, it is shifted to priority level 2, and during night time it is designated the lowest priority (level 3).

### 4.1.5 Load Shedding Scheme

As previously mentioned in Section 2.9, the CBEMA introduced a voltage sag susceptibility curve for electronic equipment [1].

The CBEMA curve defines acceptable voltage sag levels based on both the depth of the voltage sag and its duration. The curve suggests that equipment can typically handle a voltage sag from 0.9 pu to 0.8 pu for a range of 0.5 to 10 seconds. A sag from 0.8 pu to 0.7 pu may only be tolerated for about 0.5 seconds, and durations below 0.7 pu become very brief, typically around 0.02 seconds.

The load shedding scheme consists of three different levels, and the operation is determined based on the sag level (voltage sag levels are defined according to the IEEE 446 standard) [24].

Since the Level 1 shedding scheme operates within a time range of 0.5-10 seconds, the load shedding scheme consists of 8 shedding stages. According to Table 4-1, each stage executes and monitors whether the voltage sag is recovered. These stages continue until the last stage. If the voltage sag is not recovered by the last stage, the connected load is flagged, indicating that this large machine cannot be connected at the moment.

The second level comprises only three stages due to its time range of 0.5 seconds. If the voltage sag is not recovered until the last stage, the load is flagged, and the connection is not established. In the case of a level 3 voltage sag occurrence, this load is directly flagged.

Table 4-1 Load shedding scheme

| Level | Voltage sag Level | Load Shedding Scheme |
|---|---|---|
| 1 | 0.9-0.8 | Stage 1: P3-L Dimming up to 20%<br>Stage 2: P3-H<br>Stage 3: P3-L<br>Stage 4: P3-O<br>Stage 5: P2-H<br>Stage 6: P2-L<br>Stage 7: P2-O<br>Stage 8: Flag the connecting load |
| 2 | 0.8-0.7 | Stage 1: P3<br>Stage 2: P2<br>Stage 3: Flag the connecting load |
| 3 | Below 0.7 | Stage 1: Flag the connecting load |

### 4.1.6 Typical Response Time

As indicated in Table 4-2, given the typical latency associated with the most common communication protocols in the utility industry. To ensure effective execution, analysing the minimum duration of required data is crucial. This analysis considers latency, processor processing time, and the time needed for physical link conversion. A delay time of 100 milliseconds is considered in the load shedding scheme for optimal performance. This indicates that every execution is performed by analysing a minimum of 100 milliseconds of data.

Table 4-2 Typical latencies of communication protocols [25]

| | Latency (Typical values) |
|---|---|
| IEEE C37.118 | <1 ms |
| IEC 61850 | 4 ms |
| IEC 60870-6 | ~10 ms |
| DNP3 | 10-50 ms |

### 4.1.7 Restoration Scheme

The Restoration Scheme is a comprehensive strategy designed to restore all loads to normal operation. It achieves this by carefully monitoring the voltage at each load point when each load is connected.

Table 4-3 Restoration Plan

| Step | Connecting Load Category |
|---|---|
| 1 | P1 |
| 2 | P2 - O |
| 3 | P2 - H |
| 4 | P2 - L |
| 5 | P3 – O |
| 6 | P3 – H |
| 7 | P3 - L |

As shown in Table 4-3, the Restoration Scheme consists of seven steps that are initiated when the voltage at each load point returns to its normal range.

Following voltage recovery after the load shedding algorithm execution, the restoration scheme implements a 200 ms wait time to allow for voltage stabilization before initiating the restoration process. This ensures the voltage level remains within acceptable limits before proceeding to the next.

Loads are then reconnected to the system in a staged manner, one step at a time. During each step, the voltage magnitude at each bus (load point) is monitored to verify restoration without voltage sag. After each stage is completed, a verification process confirms voltage stability before proceeding to the subsequent stage.

The load-shedding scheme prioritizes ongoing shedding scheme. If a load connection attempt occurs during the process, it is deferred until voltage sag has fully recovered. The deferred load is then integrated following the established restoration sequence.

If a large machine causes a significant voltage sag in the system, the load will be flagged in the algorithm. Consequently, the operation of those machines will be restricted within a given period. This approach ensures that each step of the restoration process is executed with precision, emphasizing thorough monitoring, verification, and strategic management of loads to prevent any recurrence of voltage sag.

## Integrated System Operation

The uniqueness of the load management scheme lies in its ability to recognize when a load connects to the system. Upon connection, the system promptly identifies the newly connected load and keeps track of the total number of connected loads at any given moment. This approach ensures that the system remains unresponsive to abnormalities such as short circuits and overcurrent faults that may occur independently of new load connections.

The Decoupled Double Synchronous Reference-Based Phase-Locked Loop is a key feature, enabling the inverter to control both positive sequence and negative sequence voltages during voltage unbalances. This functionality enables the inverter remains connected and provides support to the grid during both balanced and unbalanced

conditions. In this approach, whenever a voltage sag occurs, it provides grid support regardless of whether it is due to an unbalanced fault or load connection.

# CHAPTER 5

# UNBALANCED INVERTER OPERATION

## Unbalanced Inverter Operation

An example case is provided in this section to illustrate how the inverter's unbalanced operation is executed. At this point, the fault level of the distribution system is selected to demonstrate the characteristics of a weak grid. The inverter size is selected so that it can make a noticeable contribution to restoring the system. In this section, a commonly used multilevel inverter, specifically a 5-level diode-clamped inverter, is utilized. The system's unbalanced state was created by creating an unbalanced fault, as shown in Figure 5-1.

- Fault Level of the Grid: 10 MVA
- Capacity of the Battery Energy Storage System (BESS): 1000 Ah
- Inverter Type: 5-Level Diode-Clamped Inverter

In Chapter 2, the Flexible Positive and Negative Sequence Current (FPNSC) strategy was introduced. This strategy allows for the adjustment of coefficients $k_1$ and $k_2$ defined in (2-5) and (2-6) to control the ratio between positive and negative sequence currents based on the operational philosophy and the requirements for active and reactive power. However, in this particular study, coefficient $k_1$ can be disregarded. Since the total power delivered to the grid solely targets voltage restoration at the PCC, $k_1$ effectively becomes zero. Consequently, only reactive current injection is necessary for the grid.

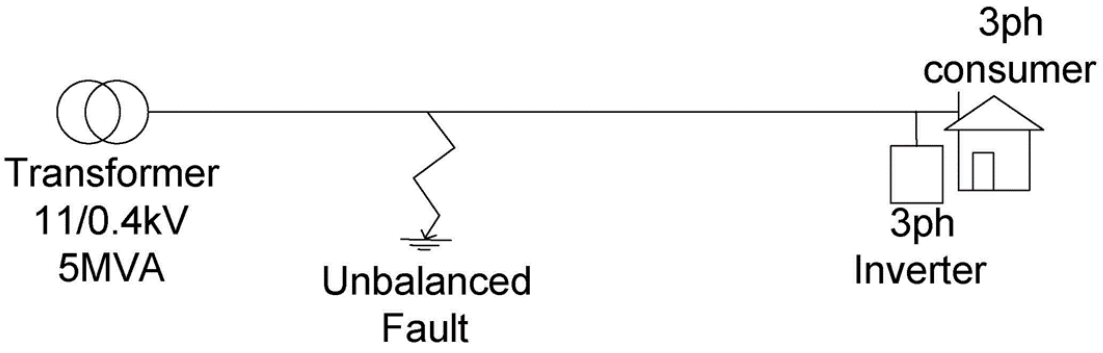


Figure 5-1 Unbalanced fault

The value of $k_2$ plays a critical role in this study. It determines the composition of the reactive currents injected into the grid, specifically in terms of their positive and negative sequence components. This, in turn, influences the effectiveness of voltage restoration at the PCC.

The system model is shown in Figure 5-2, where the FPNSC strategy is configured to inject the maximum positive-sequence reactive current that the power converter can deliver. Figure 5-3 shows the grid voltage at the PCC without inverter support, while Figure 5-4 illustrates voltage improvement at the inverter bus with inverter support.

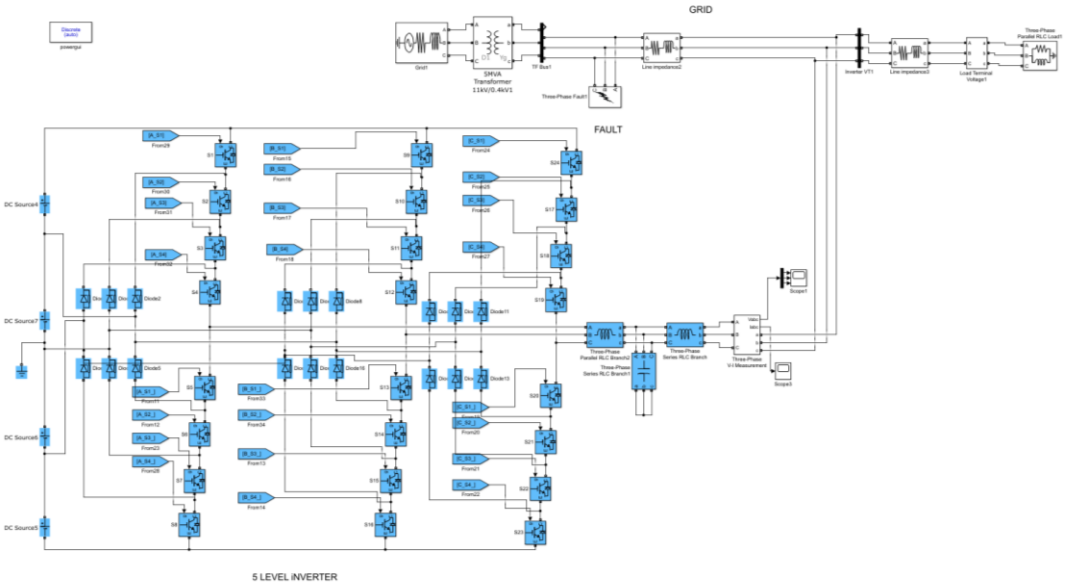


Figure 5-2 Matlab model for the general system

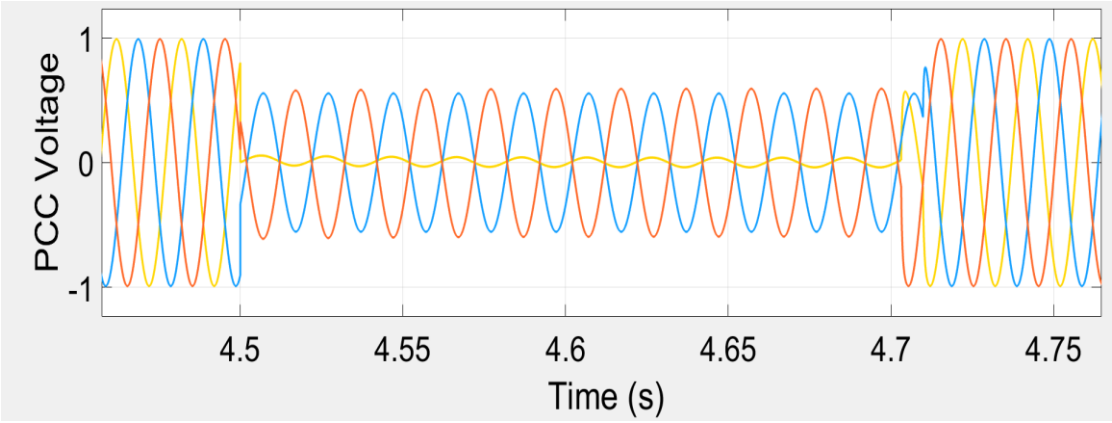


Figure 5-3 The unbalance occurrence with absent inverter support

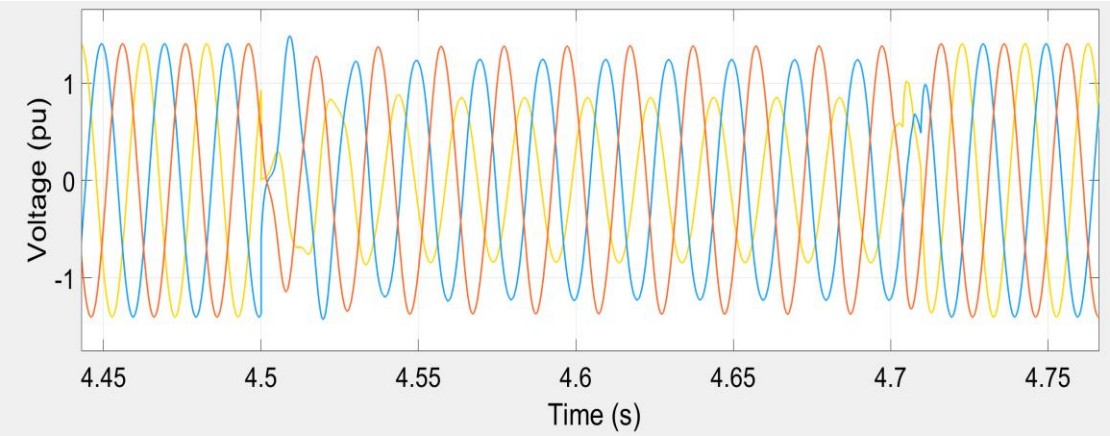


Figure 5-4 The unbalance occurrence with inverter support

## Summary

Grid faults can cause unbalanced voltages, harming connected power converters. To prevent this, special controlling method are needed to avoid the inverter disconnection even when the grid voltage is unbalanced.

Decoupled Double Synchronous Reference Frame Phase-Locked Loop (DDSRF-PLL) systems provide accurate measurements of positive and negative sequence components, facilitating effective inverter control.

Several control structures are available for injecting symmetrical components based on the active and reactive power requirements. One of the most advanced strategies is the Flexible Positive and Negative Sequence Control (FPNSC) strategy. In this study, FPNSC is employed with the control on the maximum current where it limits the current drawn at the output to ensure, current does not exceed the IBR's nominal value.

# CHAPTER 6

# COST OF IMPLEMENTATION

## Typical Implementation Cost

The cost of implementing this system depends on two factors: the size of the distribution system and the existing features it includes. Utilizing existing demand-side management infrastructure, local control centres, databases, and communication platforms can help reduce costs and integrate additional features with other systems. Table 6-1 shows the unit costs of some of the major items included in this system.

The items in Table 6-1 can be used to implement a system in smaller-scale distribution systems. When changes occur in the size of the distribution system, the consideration of incorporating more advanced components to effectively handle and control the proposed load management schemes would be necessary.

Table 6-1 Typical System Implementation Component Cost

| Component | | Product | Per unit Percentage cost | Unit Cost |
|---|---|---|---|---|
| Micro Processor | | STM32 | 1.7% | Rs.2,200.00 |
| Central Server and Database System | | Hpe Proliant Server G10 | 46.15% | Rs.60,000.00 |
| | Communication Gateway | MQTT 3100 Edge Computing Gateway | 45.69% | Rs. 59,400.00 |
| | Communication Hardware | SIM7028 NB-IoT | 3.6% | Rs 4,620.00 |
| The Cost For CTs And VTs | | Power Meter RS485 | 2.9% | Rs 3,900 –Rs 11,000 |

This system is particularly suited for weak grids, as utilities can evaluate its impact on connected consumers regarding voltage sag and the consequent financial and economic losses. Implementation decisions can be based on this evaluation. Unbalanced operation of the inverters can significantly contribute to issues in such weak grids. Additionally, even off-grid distribution systems can be benefited from incorporating this system, as it can help reduce power quality problems experienced by consumers.

# CHAPTER 7

# IMPLEMENTATION OF THE PROPOSED METHOD

## Case Study 1

In Case Study 1, only the operation of the load management scheme was considered. The chosen scenario involves a factory facing voltage sags due to the operation of its large machine. The relevant system data includes a fault level at the 11 kV Bus of 18.5 kA, a 11/ 0.4 kV transformer with a rating of 100 kVA, and a cable consisting of an Aerial Bundle Conductor with a cross-sectional area of 70 $mm^2$. The largest machine is a 7.5 kW rated induction motor. Figure 7-1 illustrates the ETAP model of the single-line diagram, indicating the location of the large machine and providing an overview of the total system schematic.

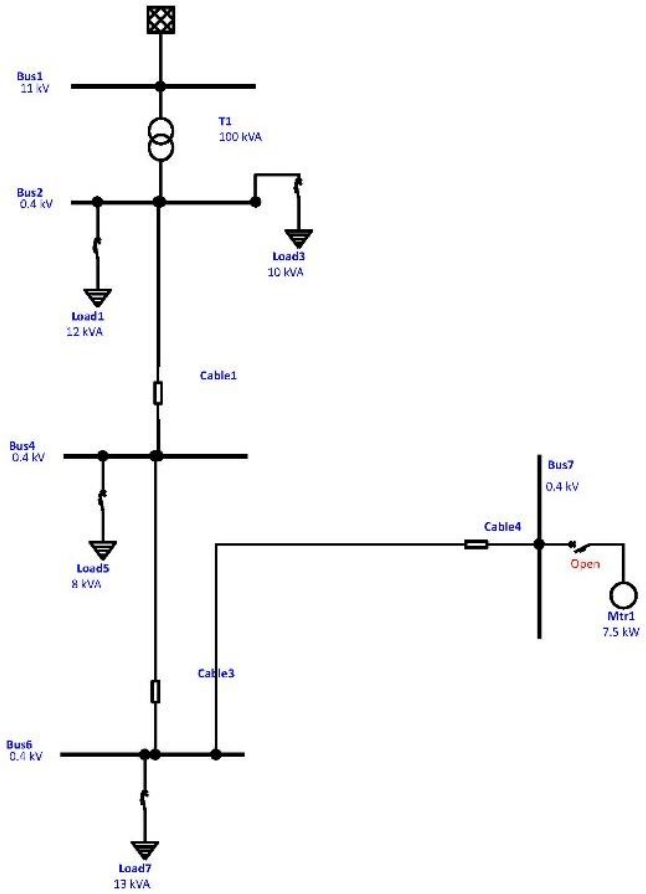


Figure 7-1 ETAP model for case study 1

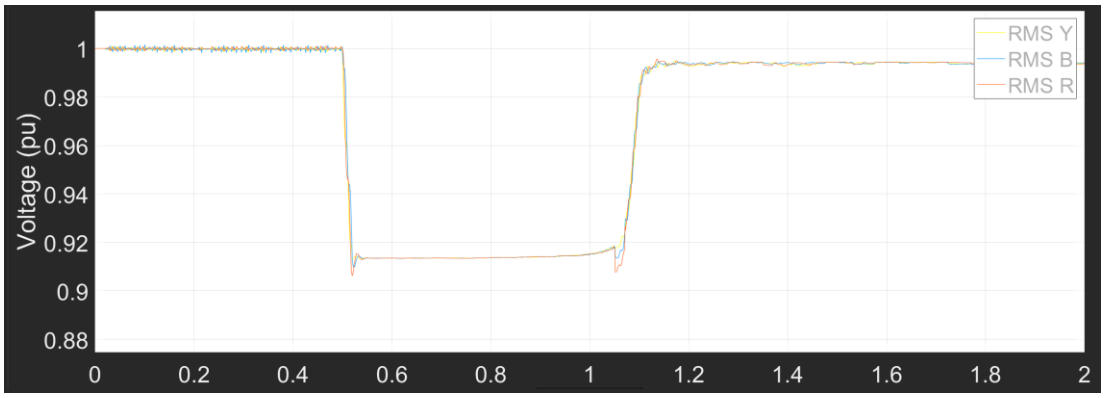


Figure 7-2 Operating a large induction machine within a distribution system under light load condition

As illustrated in Figure 7-2, operating the large machine under lightly loaded conditions allows it to be started without exceeding the voltage sag limit. However, as shown in Figure 7-3, when the overall system load reaches up to 50% of its capacity, voltage sags occur ranging between 0.9 to 0.8.

This observation implies a correlation between the increasing load on the system and the occurrence of voltage sag, particularly when starting the large induction machine. Understanding this relationship is crucial for developing effective load management strategies to mitigate voltage sag issues in the operational environment. By identifying the critical load thresholds and their impact on voltage stability, specific measures can be implemented to optimize system performance and ensure the seamless start of large machines within acceptable voltage levels.

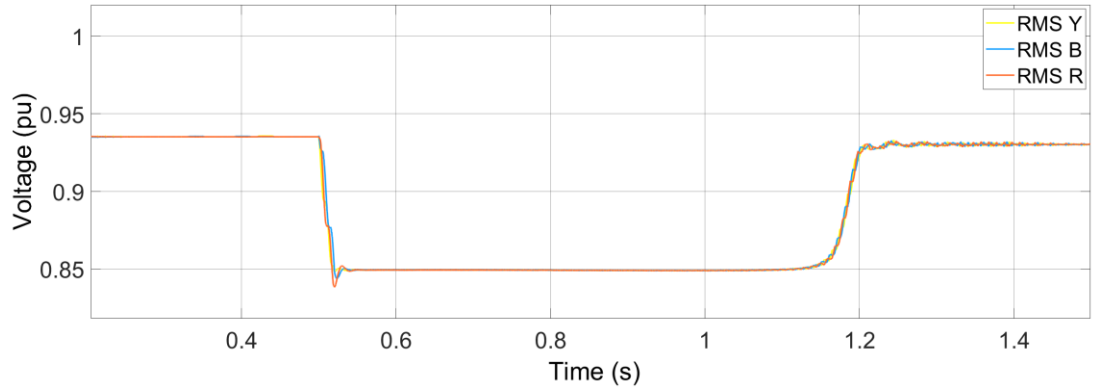


Figure 7-3 Operating a large induction machine within a distribution system under 50% load condition

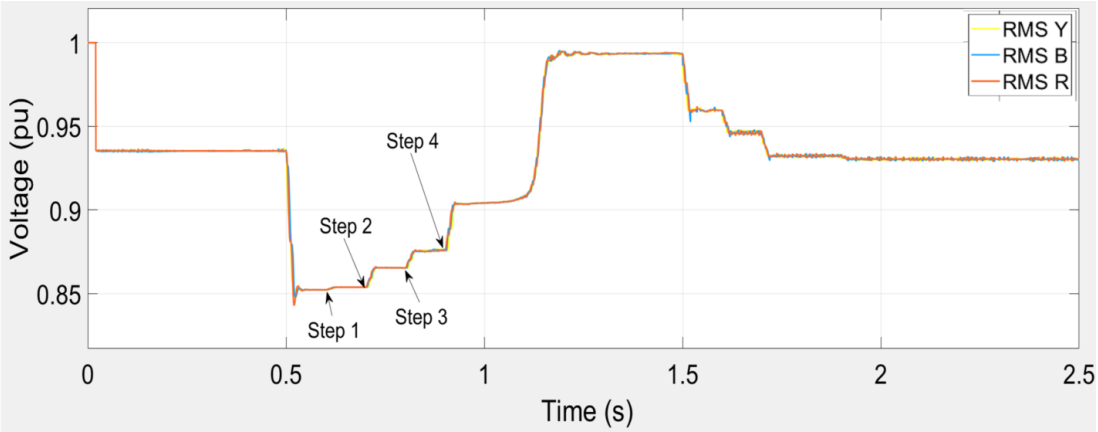


Figure 7-4 Load management scheme operation

The implemented load management scheme demonstrates its effectiveness in rapidly recovering voltages during voltage sag events. As illustrated in Figure 7-4, the scheme can restore voltage less than 0.4 seconds. This rapid response is crucial for mitigating the impact of voltage sags on sensitive equipment.

The severity of a voltage sag is categorized based on the rms voltage level. In this scenario, the voltage sag falls within the range of 0.9 pu to 0.8 pu, corresponding to sag level 1 as defined in Table 4-1. This category typically consists of multiple stages with predetermined load shedding strategy.

The load management scheme operates by sequentially shedding non-critical loads in stages. Once a specific stage successfully restores the voltage to an acceptable level, the load shedding process stops at that stage.

Table 7-1 Load shedding scheme operation

| Step | Connecting Load Category |
|---|---|
| 1 | P1 |
| 2 | P2 - O |
| 3 | P2 - H |
| 4 | P2 - L |
| 5 | P3 – O |
| 6 | P3 – H |
| 7 | P3 - L |

Table 7-2 Load restoration execution

| Level | Voltage sag Level | Load Shedding Scheme |
|---|---|---|
| 1 | 0.9-0.8 | Stage 1: P3-L Dimming up to 20%<br>Stage 2: P3-H<br>Stage 3: P3-L<br>Stage 4: P3-O<br>Stage 5: P2-H<br>Stage 6: P2-L<br>Stage 7: P2-O<br>Stage 8: Flag the connecting load |
| 2 | 0.8-0.7 | Stage 1: P3<br>Stage 2: P2<br>Stage 3: Flag the connecting load |
| 3 | Below 0.7 | Stage 1: Flag the connecting load |

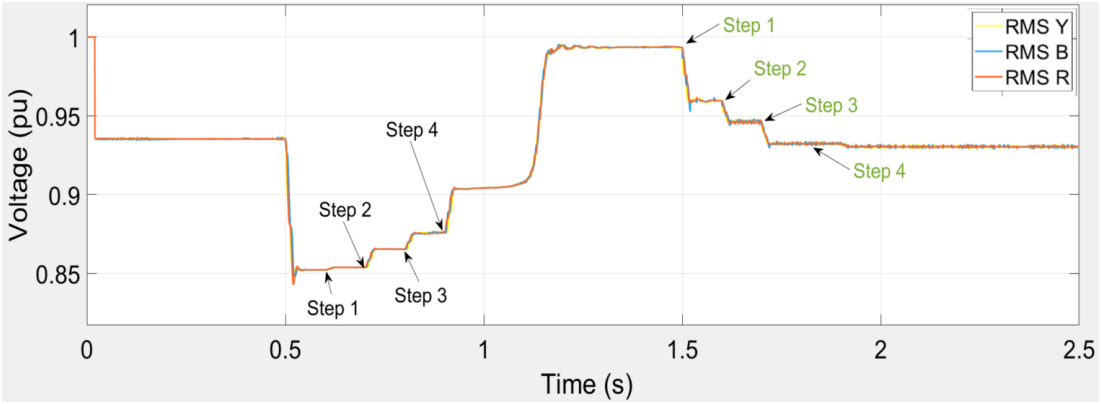


Figure 7-5 Load restoration execution

In this case study, the scheme efficiently recovered from the voltage sag by executing only four stages of load shedding.

According to Table 7-1, it is evident that P3-L (20%), P3-H, P3-L, and P3-O operated in the load shedding scheme. Thus, it can be observed that only priority scheme 3 loads are being shed.

Therefore, during the restoration scheme operation, there is no need to start from step 1 since steps 1 to 4 were not operated during the load shedding scheme. Instead, as shown in table 7-2, the operation begins from step 5, gradually adding each step while monitoring the voltage stability at each stage, as shown in Figure 7-5. The complete execution of the algorithm, along with the restoration scheme, is shown in Figure 7-5.

Appendix A presents the varying loading of the distribution system and the induction machine starting conditions. It includes analysis of bus voltage, motor current, motor

speed, slip variation, and different bus voltage variations using ETAP. This analysis is conducted for both light loaded and conditions loaded with 50% or more, to examine the variation of the aforementioned factors with the loading.

### 7.1.1 Summary

The LMS algorithm aims to rapidly recover voltage levels within the grid, minimizing potential harm to connected equipment. Figure 7-6 depicts a scenario without the algorithm, where voltage recovery takes more than 0.7 seconds. In contrast, Figure 7-5 demonstrates that the algorithm successfully reduces the recovery time to less than 0.4 seconds. This faster recovery time minimizes the duration of voltage sag exposure for sensitive equipment, enhancing overall grid resilience.

While the case study presented here showcases a recovery time improvement from 0.7 seconds to less than 0.4 seconds, the LMS algorithm can handle scenarios with longer inrush times, such as those involving arc furnaces or large pumps.

$$E_{VS} = \int_0^T 1 - \left\{\frac{V(t)}{V_{nom}}\right\}^2 dt \qquad (7\text{-}1)$$

Where:

- $V(t)$ is the rms voltage during the voltage sag event
- $V_{nom}$ is the nominal voltage.
- $T$ is the duration of voltage sag

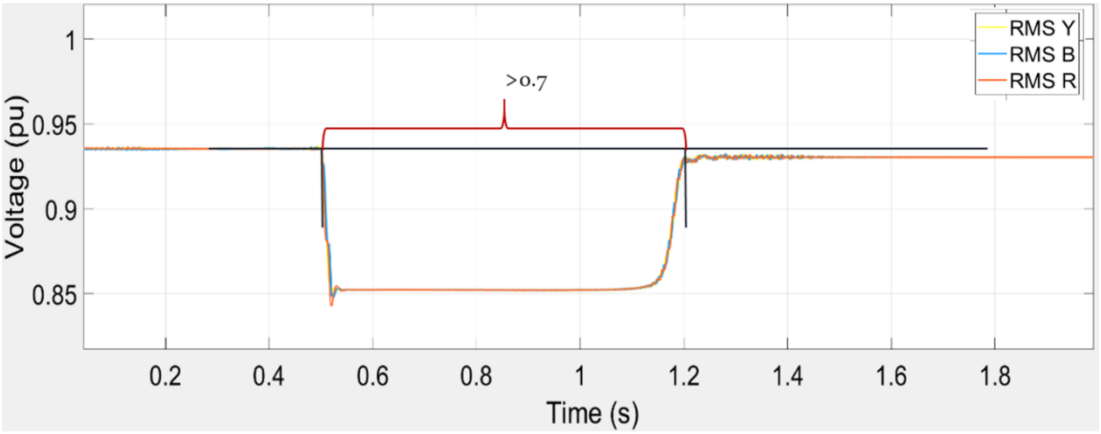


Figure 7-6 Without load management scheme

The voltage sag energy index (VSEI), as defined in (7-1), serves as a metric to quantify the voltage sag impact of a voltage sag event (26). By calculating the voltage sag energy index with and without the proposed load shedding scheme, can quantify the scheme's effectiveness in mitigating the severity of voltage sags. In this case study, the VSEI without the scheme is 206 ms, whereas with the scheme implemented, the VSEI is significantly reduced to 90.59 ms. This substantial decrease highlights the algorithm's capability to minimize the overall impact of voltage sag events on the grid.

### 7.1.2 Techno-Economic Analysis

Many weak distribution systems can adopt the load management-based sag mitigation system to reduce the impact of voltage sag. This method offers significant technical, economic, and customer satisfaction benefits. The following presents a techno-economic analysis of the Load Management-Based Sag Mitigation System, focusing on its potential to reduce voltage sag severity, improve power quality, increase reliability, lower equipment damage costs, enhance productivity, boost customer satisfaction, minimize lost revenue during voltage sag events, and mitigate the cost of total system failure.

i. The LMS prevents exposure to voltage sags beyond acceptable time limits, thus minimizing stress on electrical equipment.
ii. The LMS enhances overall power quality, leading to minimal system malfunctions and disruptions.
iii. Mitigating voltage sag severity leads to less equipment wear and tear, with minimal repair and replacement costs.

iv. Mitigating voltage sag severity ensures uninterrupted operations, minimizing production losses and downtime costs.

v. Enhanced power quality improves customer experiences and reduces complaints.

vi. Prevent voltage sag induced shutdowns leading reduced direct revenue losses during such events

From an economic perspective, the Load Management Based Sag Mitigation System proves to be a cost effective investment by directly curbing equipment damage costs. This translates into reduced expenses for repairs and replacements.

However, implementing and maintaining the LMS infrastructure, including sensors, communication systems, and control software, involves upfront costs.

Considering this upfront and the maintenance cost Table 7-3 presents an economic analysis done for case study 1.

Table 7-3 Economic analysis for case 1

| Parameter | Annual Cost | | Value |
|---|---|---|---|
| Technical benefits | | | |
| Reduced voltage sag severity | | | |
| Improved power quality | | | |
| Increased reliability | | | |
| Economic benefits | | | |
| Reduced equipment damage costs | 100,000.00 | 95% | 95,000.00 |
| Improved productivity | 500,000.00 | 95% | 475,000.00 |
| Increased customer satisfaction | | | |
| Economic risks | | | |
| Lost revenue during voltage sag events | 1,000,000.00 | 95% | 950,000.00 |
| Cost of Total system failure | 1,500,000.00 | 95% | 1,425,000.00 |
| Assumptions | | | |
| System lifetime | | 10 years | |
| Discount rate | | 15% | |
| Total system cost | | | 1,000,000.00 |
| Calculations | | | |
| Lifetime benefits | | | 29,450,000.00 |
| Discounted benefits | | | 14,780,273.60 |
| Net present value (NPV) | | | (14,780,273.60) |
| Payback period | | | 10 |
| IRR | | | 294.5% |

This evaluation considers both the revenue lost due to voltage sags and the cost of total system failure caused by voltage sag events. However, the actual revenue loss may

vary based on the impact experienced by factories or customers. If a company has data on the frequency and amount of revenue loss due to voltage sags, they can implement this load management system accordingly.

## Case Study 2

### 7.1.3 Load Management Scheme Operation

The case study 2 involved the simulation of a real distribution system in Sri Lanka that utilized inverter based resources. Simulations were conducted for both the LMS and scenarios involving the unbalanced operation of inverters on the same distribution system. To demonstrate the characteristics of a weak distribution system, the fault level at the PCC was reduced from 25 kA to 15 kA.

The evaluation of the reduction in voltage sag severity was conducted using the VSEI.

For the analysis of the implemented system operation, a small distribution system in Pahala Bomiriya, Sri Lanka, has been selected, as shown in Figure 7-8.

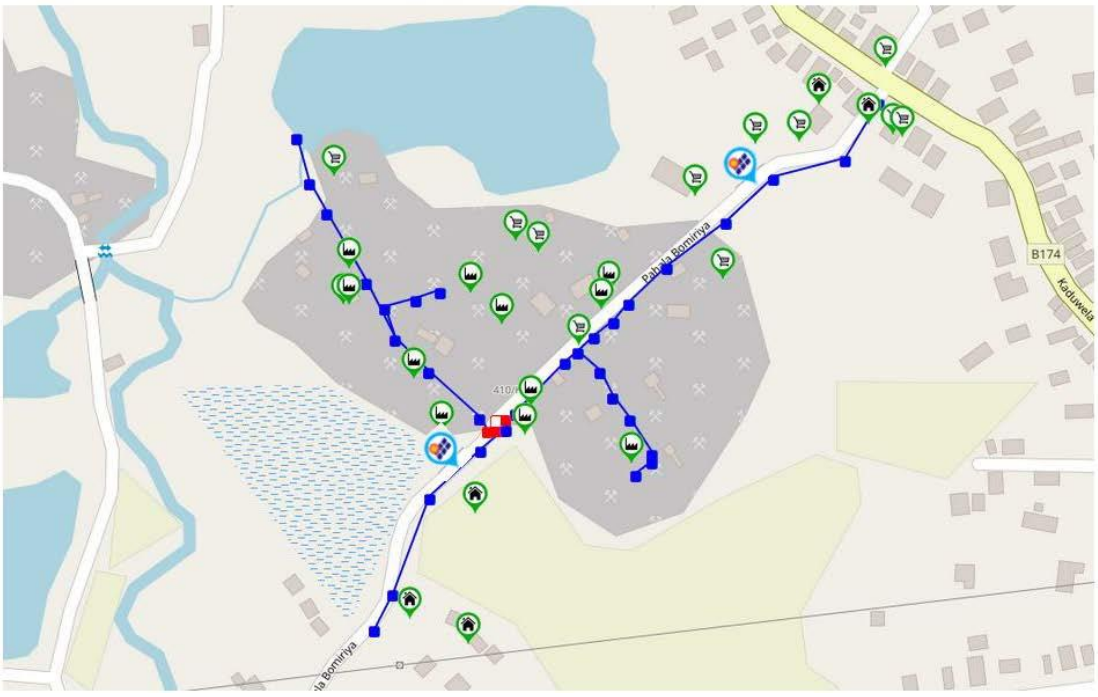


Figure 7-7 Geographical view of the distribution system (Location: Pahala Bomiriya)

Table 7-4 System data

| PCC Details | |
|---|---|
| Substation type | Bulk and Distribution |
| TF Capacity | 400 kVA |
| MV side Voltage | 33 kV |

The considered network is composed of two three-phase solar PV systems and system data is shown in Table 7-4.

The selected distribution system was comprised of various consumer types, and Table 7-5 displays the number of consumers in each category as of September 2023.

Based on the geographical locations of each consumer, the entire distribution system was modelled using MATLAB Simulink to generate different scenarios. The model of the total system using MATLAB is shown in Figure 7-9, and using this model, the operation of the large machine in this system was simulated first.

Table 7-5 Consumer details of the selected system

| Customer Type | Number of Customers |
|---|---|
| 15 A -1p | 1 |
| 30 A -1P | 12 |
| 60 A-1P | 1 |
| 60 A-3p | 7 |
| 30 A-3p | 5 |
| 15 A-3P | 2 |
| Total | 28 |

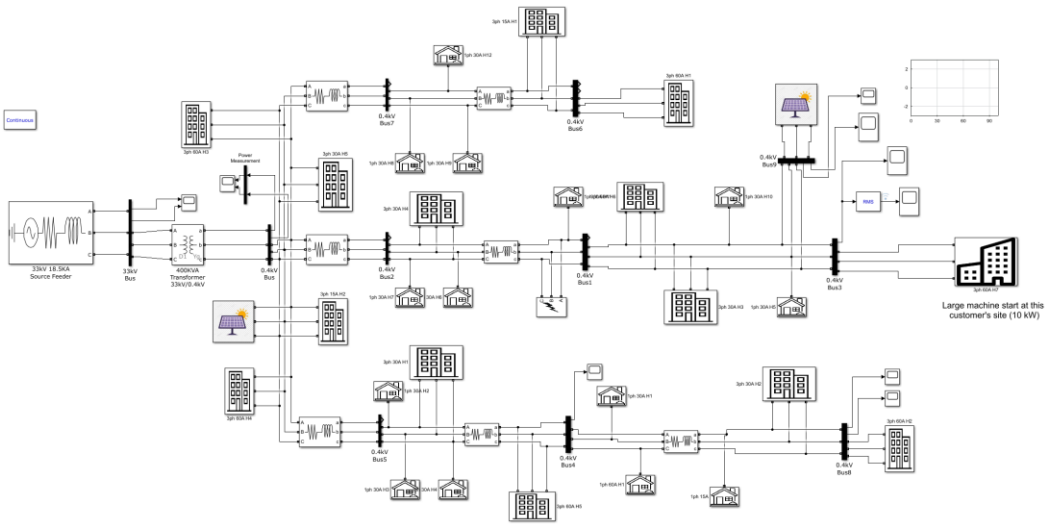


Figure 7-8 Matlab model of the selected distribution system

As illustrated in Figure 7-10, a significant voltage sag occurs at the load PCC when the large machine is operational. The measured voltage sag reaches approximately 0.85 pu and lasts for about 0.7 seconds. This voltage sag can potentially harm sensitive equipment connected to the grid.

To evaluate the effectiveness of the load shedding scheme, the VSEI is calculated with and without the scheme implemented.

The results reveal a substantial difference in the VSEI values. Without the scheme, the VSEI is observed to be 169.26 ms as per (7-1). In contrast, with the scheme implemented, the VSEI is significantly reduced to 65.02 ms. This substantial decrease highlights the algorithm's capability to mitigate the severity of voltage sags.

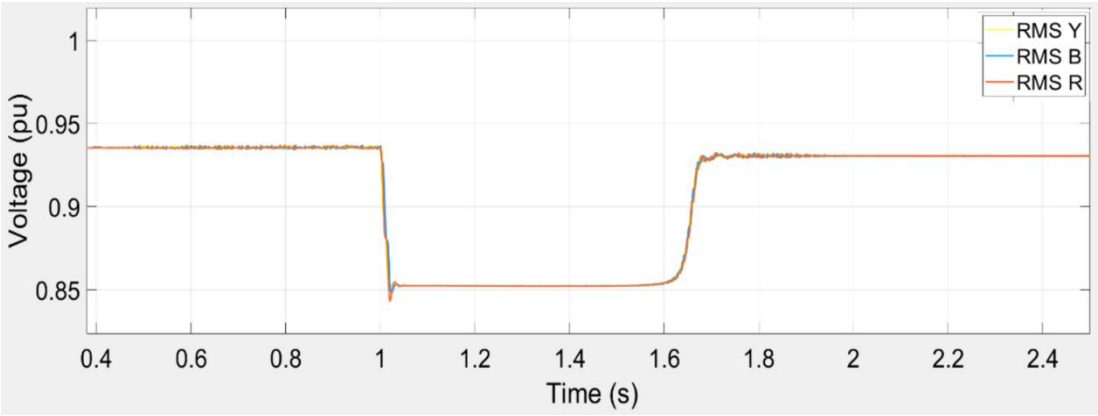


Figure 7-9 Voltage at the load PCC

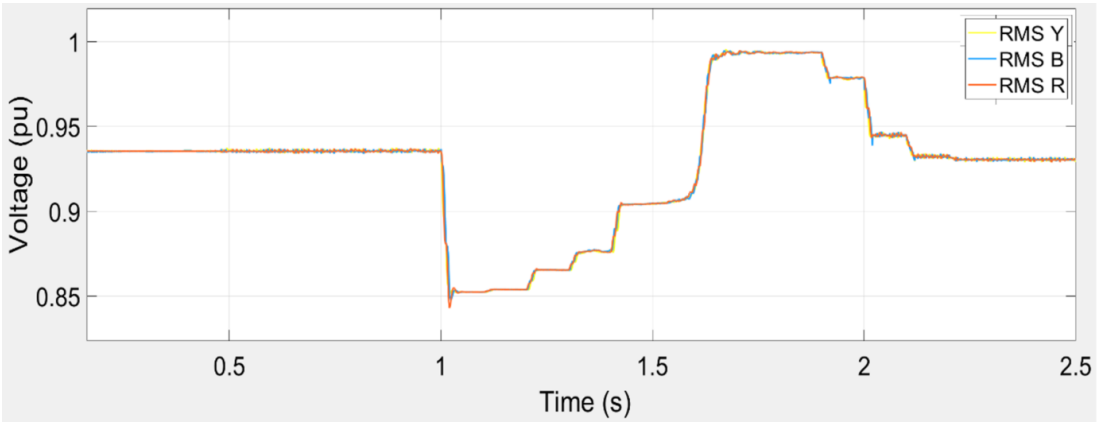


Figure 7-10 Voltage recovery by using the LMS

### 7.1.4 Inverter Unbalanced Operation

The operation of inverters under unbalanced voltage sag conditions is considered in this section. Here, the unbalanced voltage sag was induced by an L-L-G fault, as shown in Figure 7-12, and the terminal voltage of the load end inverter observed is shown in Figure 7-13.

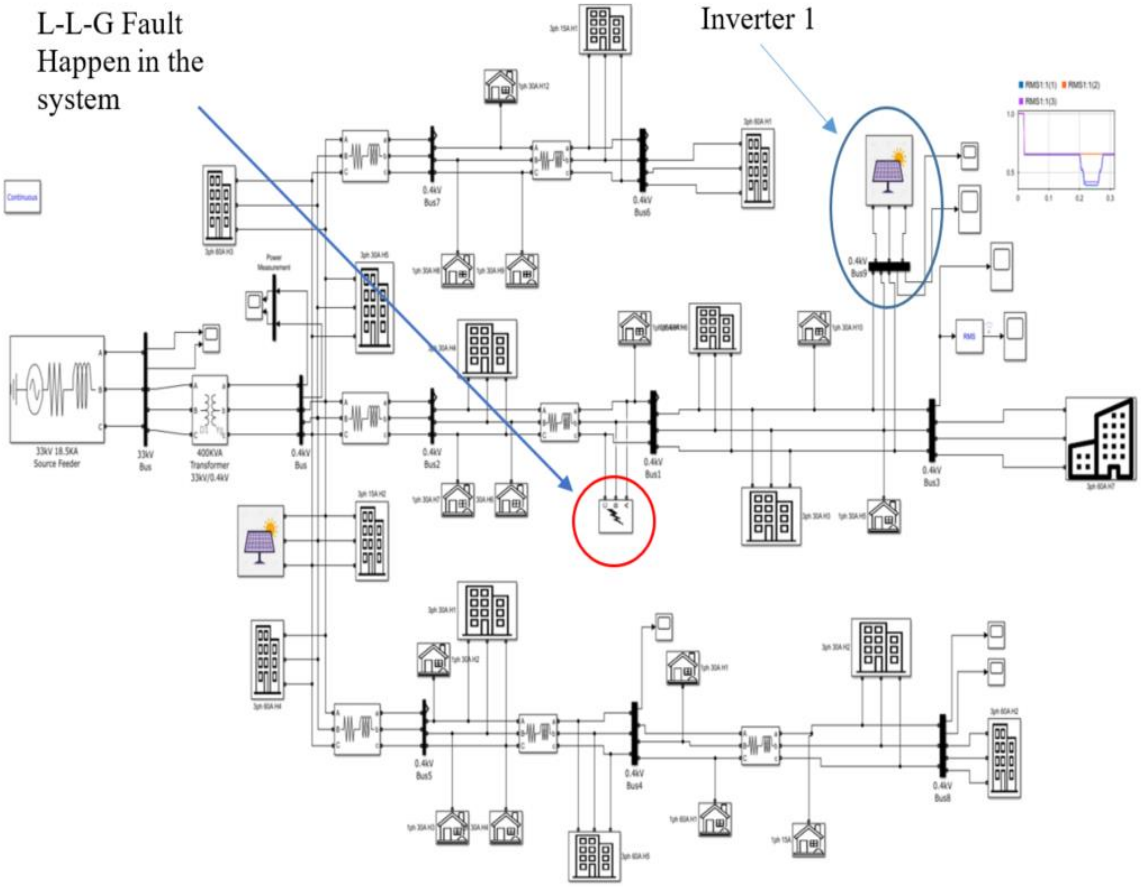


Figure 7-11 Unbalanced fault at the selected distribution system

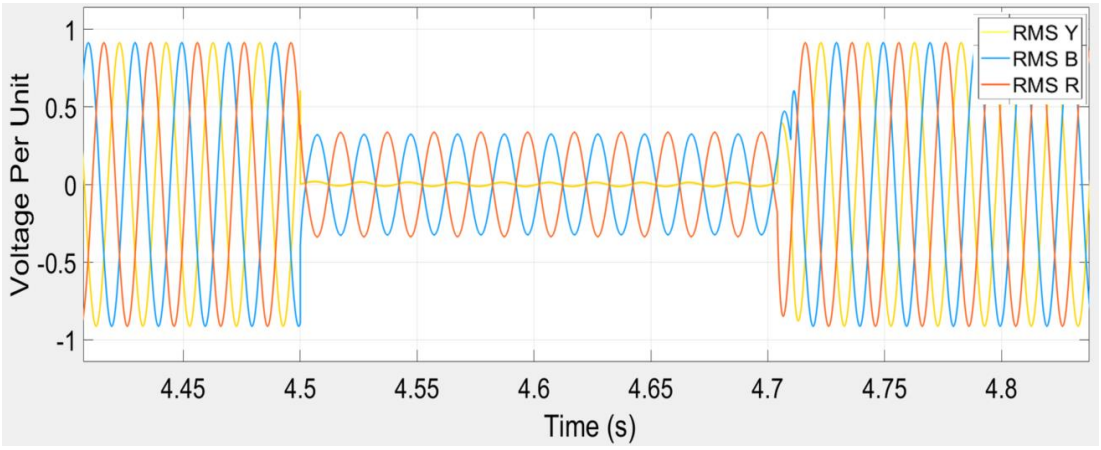


Figure 7-12 Inverter 1 terminal voltage without inverter support

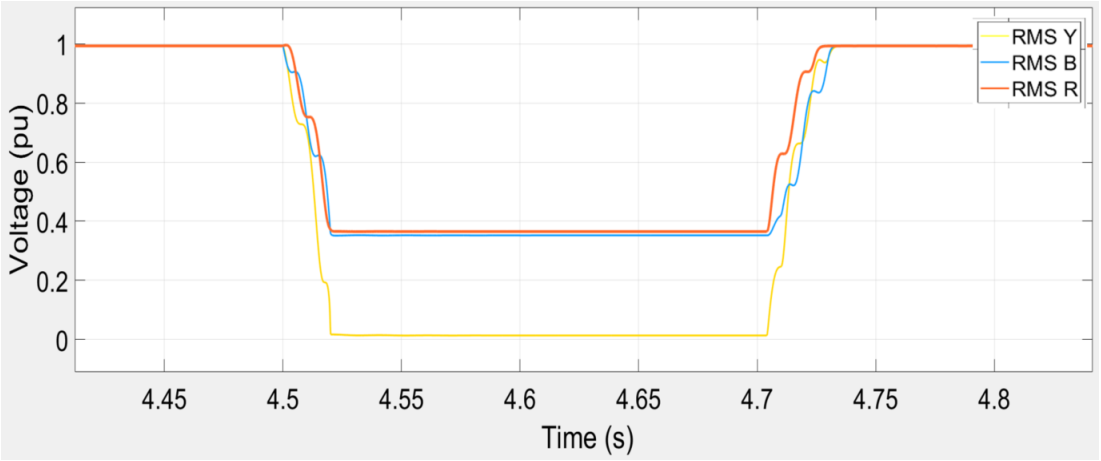


Figure 7-14 RMS phase voltages during the voltage sag without unbalanced support from the inverter 1

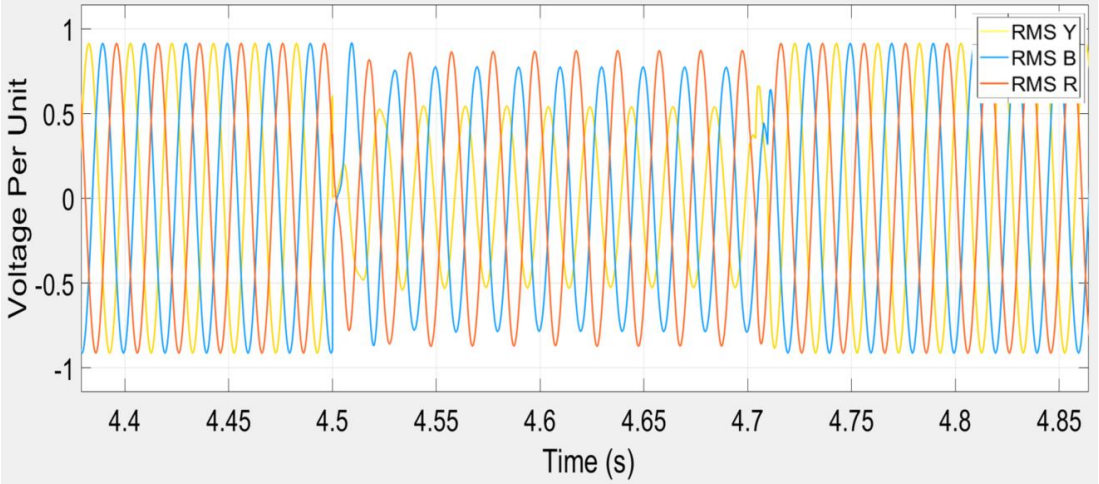


Figure 7-13 Phase voltages during the voltage sag with unbalanced support from the inverter 1

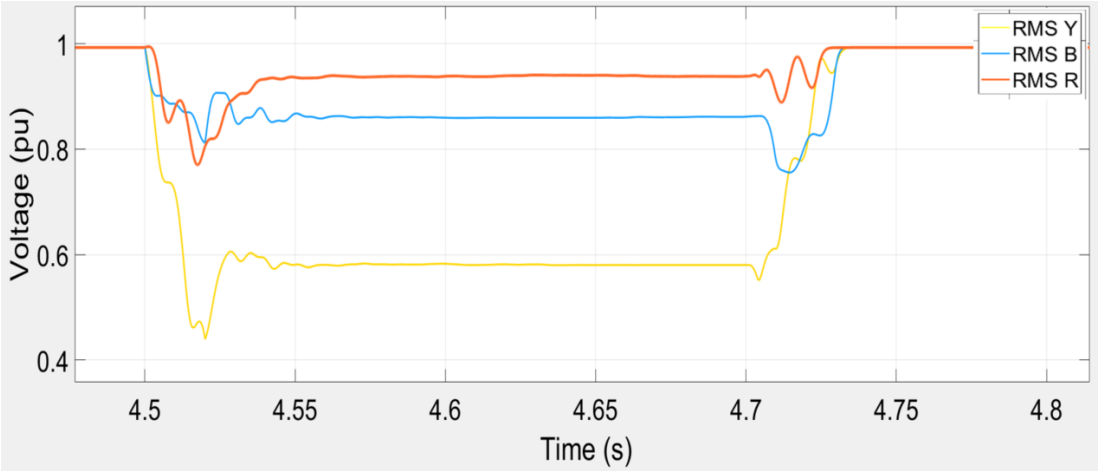


Figure 7-15 RMS phase voltages during the voltage sag with unbalanced support from the inverter 1

The Figure 7-13 clearly shows a significant voltage unbalance and sag at the inverter PCC. This is further confirmed by the RMS voltage plots in Figure 7-14, where the R and B phases drop to around 0.4 pu, while the Y phase experiences a near-zero RMS voltage.

$$\frac{V_2}{V_1} = \sqrt{\frac{1-\sqrt{3-6\beta}}{1+\sqrt{3-6\beta}}} \qquad (7\text{-}2)$$

$$\beta = \frac{V_{ab}^4 + V_{bc}^4 + V_{ca}^4}{(V_{ab}^2 + V_{bc}^2 + V_{ca}^2)^2}$$

The calculated unbalanced factor for this scenario, as defined in IEC TR 61000-3-14, can be represented by (7-2), is 92.2% (27). This high value indicates a severe voltage unbalance, further the VSEI is 54.46 ms.

In contrast, Figure 7-15 demonstrates a significant improvement in the phase voltages at the inverter PCC when the unbalanced mitigation operation mode is activated during the voltage sag event. This improvement is also reflected in the RMS voltage of Figure 7-16. The R phase voltage increases by more than 0.9 pu, the B phase by around 0.85 pu, and the Y phase by around 0.6 pu, showcasing the effectiveness of the proposed control strategy. Figure 7-17 depicts the inverter current injection during this voltage sag event.

By integrating the proposed unbalanced mitigation control strategy with the inverter, the voltage unbalance factor is significantly reduced to 26.5%. Furthermore, the VSEI

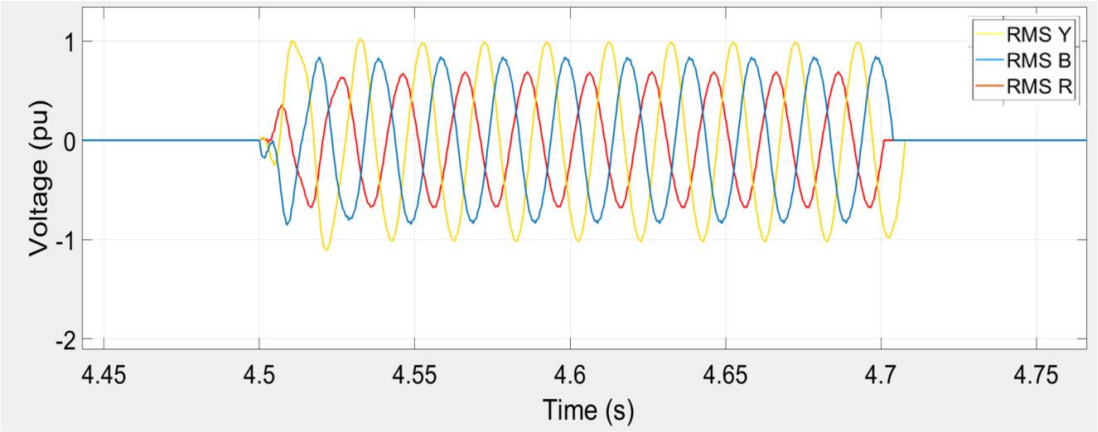


Figure 7-16 Inverter current injection during voltage unbalance

is substantially lowered to 20.08 ms. These results demonstrate the effectiveness of the inverter's unbalanced mitigation operation in voltage sag events and improving overall grid stability.

# CHAPTER 8

# CONCLUSION

This research presented a hybrid voltage sag mitigation system specifically designed for weak distribution systems with a high penetration of inverter-based resources.

*Effectiveness of the Proposed Load Management Scheme*

The effectiveness of the proposed LMS in mitigating voltage sag events was evaluated through two case studies simulating weak grid conditions.

The first case study focused on a factory experiencing voltage sag during a large motor starting event. Without the LMS algorithm, voltage recovery time was a significant 0.7 seconds. However, with the algorithm implemented, recovery time was reduced to less than 0.4 seconds. Furthermore, the voltage sag energy index, a metric quantifying the voltage sag impact, was substantially reduced from 206 ms to 90.59 ms, a decrease of over 56.1%.

The second case study investigated a real distribution system with a reduced fault level, simulating characteristics of a weak grid. Similar to the first case study, the LMS algorithm demonstrated significant effectiveness. Without the scheme, the VSEI was 169.26 ms. When the LMS was implemented, the index was reduced to 65.02 ms, reflecting a decrease of over 61.5%.

These case studies convincingly demonstrate the capability of the LMS algorithm to improve voltage recovery times and significantly reduce the overall impact of voltage sag events on the grid.

The significant improvements observed in both case studies highlight the effectiveness of the proposed load management scheme in mitigating voltage sags within weak grid environments. This approach offers a valuable tool for enhancing grid resilience and power quality.

*Effectiveness of the proposed inverter mode for mitigating unbalanced voltage sags*

Case study 2 evaluated the effectiveness of the proposed inverter control system's unbalanced voltage sag mitigation mode. This mode was tested by simulating an L-L-G fault.

Without the unbalanced voltage mitigation strategy activated, the fault resulted in a severe voltage unbalance, reflected by an unbalanced factor of 92.2%. Additionally, the voltage sag energy index, was 54.46 ms.

However, when the unbalanced voltage mitigation mode was activated, the inverter significantly improved the voltage conditions at its PCC. The unbalanced factor was substantially reduced to 26.5%. Furthermore, the VSEI was 20.08 ms.

- Over 71.1% reduction in the unbalanced factor demonstrates the effectiveness of the control system in mitigating voltage unbalance during the fault.
- A decrease of over 63.2% in the VSEI highlights the system's capability to minimize the overall impact of the voltage sag event.

The case study 2 findings demonstrate the effectiveness of the proposed inverter control system with its unbalanced voltage sag mitigation mode. This strategy offers a valuable tool for enhancing power quality in weak grids by addressing unbalanced voltage sag events and improving overall grid resilience. This approach can be particularly beneficial in systems with a high penetration of inverter-based renewable energy sources. The combined system can provide the following features.

- With the proposed load management scheme in operation, voltage recovers within CBEMA acceptable levels, mitigating undesirable exposure time to voltage sag in sensitive items.
- The proposed system significantly enhances power quality issues caused by large machine operations and unbalanced voltage sag events.
- The proposed system can utilise existing resources and offers a cost effective solution, providing an economically viable approach to address voltage sag related issues in weak grids.

Overall, the proposed system represents a cost-effective solution tailored to the challenges posed by weak grids. It offers benefits in terms of improved voltage levels, enhanced power quality, and compatibility with existing infrastructure.

## Future Improvements

While the proposed hybrid voltage sag mitigation system demonstrates significant effectiveness, further research can explore potential enhancements to its capabilities and overall performance within weak grid environments.

1. Feeder rearrangement for optimized load distribution

Distribution networks may not be optimized for handling voltage sag events. Integrating a feeder rearrangement scheme with the existing LMS holds potential for improving system strength and reliability. Feeder rearrangement involves strategically reconfiguring feeder connections within the distribution network. This optimization could involve techniques such as load balancing across feeders, reducing feeder lengths, or isolating critical loads from non-critical ones during voltage sag events. By implementing such strategies, the system can ensure a more even distribution of loads across the grid, minimizing voltage sags and improving overall system resilience.

2. Centralized BESS for enhanced resilience

Incorporating a central BESS alongside the inverter operation for unbalanced voltage sag mitigation system offers another capable way for enhancing the system's resilience. The BESS can serve as a readily available source of active and reactive power during voltage sag events. Additionally, by strategically integrating feeder rearrangement strategies with the central BESS, nearby distribution systems can be further strengthened. The BESS could be strategically located within the network to provide support to multiple feeders experiencing voltage sag events. This combined approach can enhance the overall resilience and performance of the system. However, further research is necessary to determine the optimal placement and capacity of the BESS to maximize its effectiveness within the specific weak grid environment.

These potential enhancements have the potential to further improve the capabilities of the proposed system in several key aspects:

1. Feeder rearrangement strategies can optimize load distribution across the grid, minimizing voltage drops and improving the system's ability to handle higher load demands without experiencing voltage sags.
2. Both feeder rearrangement and central BESS integration can contribute to improved system reliability. Optimized load distribution and readily available power reserves from the BESS can enhance the system's ability to maintain stable voltage levels during disturbances and ensure continuous power supply to critical loads.

By exploring these potential research directions, the proposed hybrid voltage sag mitigation system can be further refined, leading to a more robust and resilient solution for weak grid applications.

# REFERENCES


[1] “IEEE SA - IEEE 1159-2019,” IEEE Standards Association. https://standards.ieee.org/ieee/1159/6124/

[2] Bollen MH. Understanding power quality problems. In Voltage sags and Interruptions 2000 Feb. Piscataway, NJ, USA: IEEE press.

[3] S. Arias-Guzman *et al.*, "Analysis of voltage sag severity case study in an industrial circuit," *2015 IEEE Industry Applications Society Annual Meeting*, Addison, TX, USA, 2015, pp. 1-6, doi: 10.1109/IAS.2015.7356932.

[4] M. G. Dozein, P. Mancarella, T. K. Saha and R. Yan, "System Strength and Weak Grids: Fundamentals, Challenges, and Mitigation Strategies," *2018 Australasian Universities Power Engineering Conference (AUPEC)*, Auckland, New Zealand, 2018, pp. 1-7, doi: 10.1109/AUPEC.2018.8757997.

[5] https://www.saurenergy.com/solar-energy-blog/what-to-do-when-your-inverter-givesg-phase-alarm

[6] B. Soreng, R. Garnayak and R. Pradhan, "A Synchronous Reference Frame based PLL Control for a Grid-Tied Photovoltaic System," *2017 International Conference on Current Trends in Computer, Electrical, Electronics and Communication (CTCEEC)*, Mysore, India, 2017, pp. 1017-1022, doi: 10.1109/CTCEEC.2017.8455132.

[7] S. Chatterjee and S. Chatterjee, "Simulation of synchronous reference frame PLL based grid connected inverter for photovoltaic application," *2015 1st Conference on Power, Dielectric and Energy Management at NERIST (ICPDEN)*, Itanagar, India, 2015, pp. 1-6, doi: 10.1109/ICPDEN.2015.7084493.

[8] P. Rodriguez, J. Pou, J. Bergas, J. I. Candela, R. P. Burgos and D. Boroyevich, "Decoupled Double Synchronous Reference Frame PLL for Power Converters Control," in *IEEE Transactions on Power Electronics*, vol. 22, no. 2, pp. 584-592, March 2007, doi: 10.1109/TPEL.2006.890000.

[9] M. Reyes, P. Rodríguez, S. Vázquez, A. Luna, J. M. Carrasco and R. Teodorescu, "Decoupled Double Synchronous Reference Frame current controller for unbalanced grid voltage conditions," *2012 IEEE Energy Conversion Congress and Exposition (ECCE)*, Raleigh, NC, USA, 2012, pp. 4676-4682, doi: 10.1109/ECCE.2012.6342184.

[10] C. Kalaivani and K. Rajambal, "Grid Integration of Three-phase Inverter using Decoupled Double Synchronus Reference Frame PLL," *2019 International Conference on Computation of Power, Energy, Information and Communication (ICCPEIC)*, Melmaruvathur, India, 2019, pp. 221-226, doi: 10.1109/ICCPEIC45300.2019.9082386.

[11] IEEE 1547-2018: IEEE Standard for Interconnection and Interoperability of Distributed Energy Resources with Associated Electric Power Systems Interfaces

[12] IEC 61727:2004: Photovoltaic (PV) systems - Characteristics of the utility interface

[13] DIN VDE V 0126-1-1:2013-08: Automatic disconnection device between a generator and the public low-voltage grid

[14] M. H. J. Bollen and R. A. A. de Graaff, "Behavior of AC and DC drives during voltage sags with phase-angle jump and three-phase unbalance," *IEEE Power Engineering Society. 1999 Winter Meeting (Cat. No.99CH36233)*, New York, NY, USA, 1999, pp. 1225-1230 vol.2, doi: 10.1109/PESW.1999.747388.

[15] J. C. Gomez, M. M. Morcos, C. A. Reineri and G. N. Campetelli, "Behavior of induction motor due to voltage sags and short interruptions," in *IEEE Transactions on Power Delivery*, vol. 17, no. 2, pp. 434-440, April 2002, doi: 10.1109/61.997914.

[16] D. Zhang and T. Liu, "Effects of voltage sag on the performance of induction motor based on a new transient sequence component method," in *CES Transactions on Electrical Machines and Systems*, vol. 3, no. 3, pp. 316-324, Sept. 2019, doi: 10.30941/CESTEMS.2019.00042.

[17] H. Beig, S. Nema and S. K. Gawre, "Power Quality Issues and Mitigation approaches for modern power scenarios: encapsulation," 2020 IEEE International Students' Conference on Electrical,Electronics and Computer Science (SCEECS), Bhopal, India, 2020, pp. 1-6, doi: 10.1109/SCEECS48394.2020.70.

[18] IEEE 1100-2005: IEEE Recommended Practice for Powering and Grounding Electronic Equipment

[19] P. RodrÍguez, A. Timbus, R. Teodorescu, M. Liserre and F. Blaabjerg, "Reactive Power Control for Improving Wind Turbine System Behavior Under Grid Faults," in *IEEE Transactions on Power Electronics*, vol. 24, no. 7, pp. 1798-1801, July 2009, doi: 10.1109/TPEL.2009.2014650.

[20] Chen Q, Fan X, Zhang P, Fanl C. Flexible positive and negative sequence current control method and equivalent sequence network model for inverting distributed power supply [J]. Power System Protection and Control. 2018;46(14):57-62.

[21] Hossain MI, Abido MA. Positive-negative sequence current controller for LVRT improvement of wind farms integrated MMC-HVDC network. IEEE Access. 2020 Oct 20;8:193314-39.

[22] P. Rodriguez, A. Luna, J. R. Hermoso, I. Etxeberria-Otadui, R. Teodorescu and F. Blaabjerg, "Current control method for distributed generation power generation plants under grid fault conditions," *IECON 2011 - 37th Annual Conference of the IEEE Industrial Electronics Society*, Melbourne, VIC, Australia, 2011, pp. 1262-1269, doi: 10.1109/IECON.2011.6119490.

[23] M. Reyes, P. Rodriguez, S. Vazquez, A. Luna, R. Teodorescu and J. M. Carrasco, "Enhanced Decoupled Double Synchronous Reference Frame Current Controller for Unbalanced Grid-Voltage Conditions," in *IEEE Transactions on Power Electronics*, vol. 27, no. 9, pp. 3934-3943, Sept. 2012, doi: 10.1109/TPEL.2012.2190147.

[24] IEEE 446-1995 IEEE Recommended Practice for Emergency and Standby Power Systems for Industrial and Commercial Applications

[25] I. Ali, M. A. Aftab and S. M. S. Hussain, "Performance comparison of IEC 61850-90-5 and IEEE C37.118.2 based wide area PMU communication networks," in *Journal of Modern Power Systems and Clean Energy*, vol. 4, no. 3, pp. 487-495, July 2016, doi: 10.1007/s40565-016-0210-y.

[26] D. D. Sabin and M. H. J. Bollen, "Overview of IEEE Std 1564-2014 Guide for Voltage Sag Indices," *2014 16th International Conference on Harmonics and Quality of Power (ICHQP)*, Bucharest, Romania, 2014, pp. 497-501, doi: 10.1109/ICHQP.2014.6842753.

[27] IEC TR 61000-3-14:2011 Electromagnetic compatibility (EMC) - Part 3-14: Assessment of emission limits for harmonics, interharmonics, voltage fluctuations and unbalance for the connection of disturbing installations to LV power systems

## Appendix A

This appendix present the varying loading of the distribution system and the induction machine starting conditions in case study 1. It includes analysis of bus voltage, motor current, motor speed, slip variation, and different bus voltage variations using ETAP.

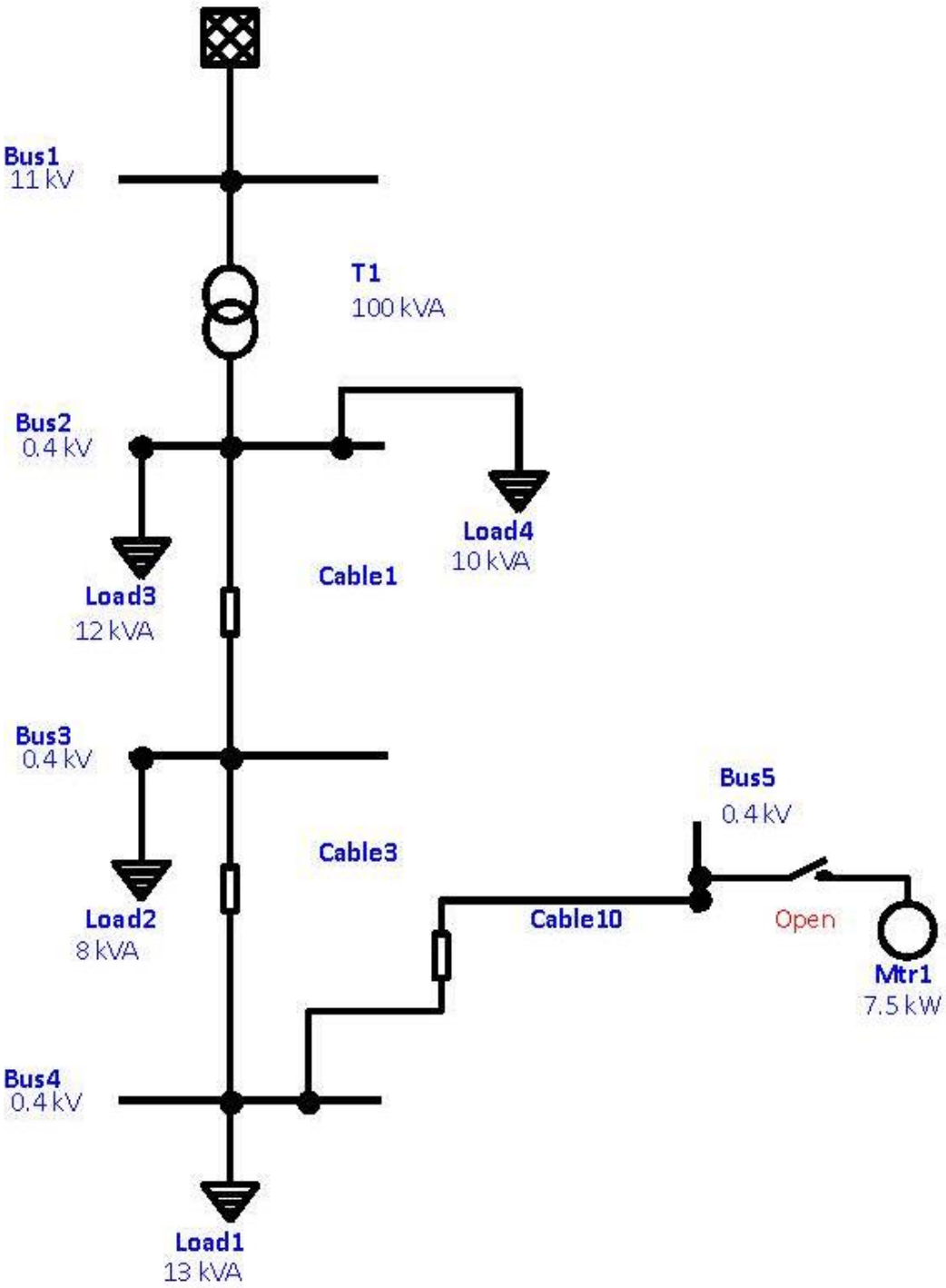


Figure A. 1 SLD of case study 1

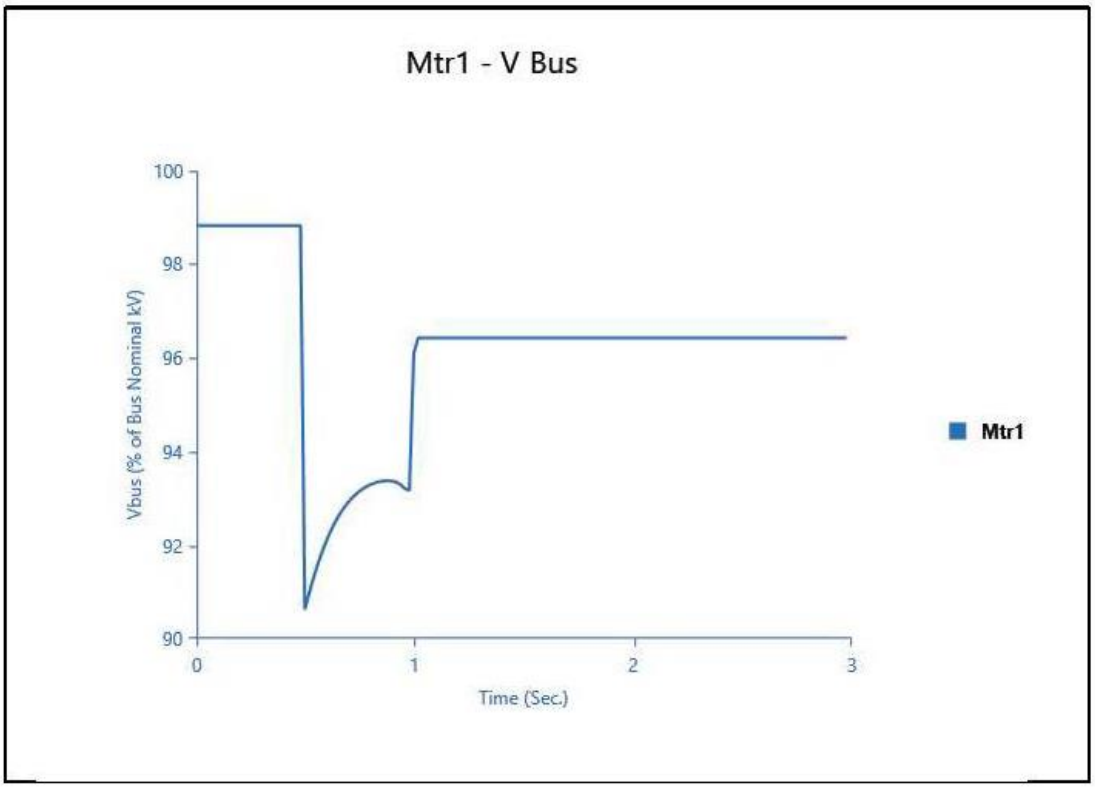


Figure A. 2 Motor PCC voltage at light load

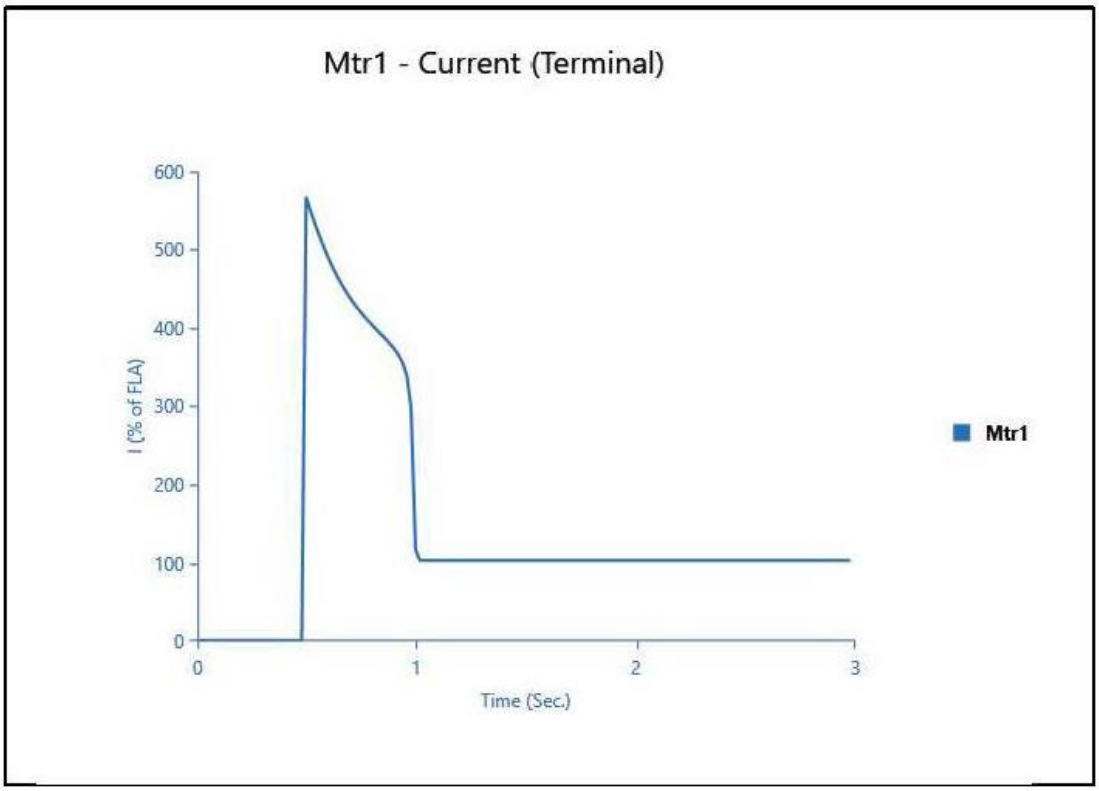


Figure A. 3 Motor terminal current during light load start-up

Figure A.1 illustrates a single-line diagram depicting the entire system analysed in Case Study 1. The initial investigation focuses on the system's behaviour under light

loading condition. Figure A.2 illustrates the voltage profile at the motor's PCC during the starting event. As depicted in Figure A.2, the motor's PCC voltage shows no voltage sag under light load condition.

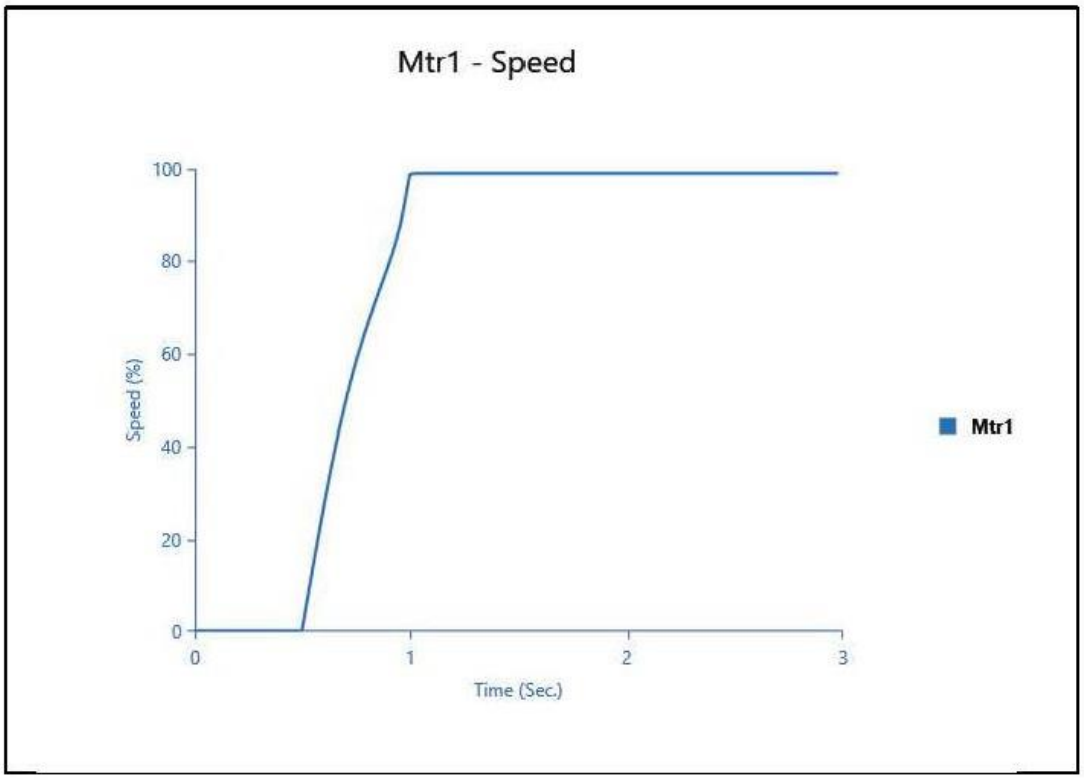


Figure A. 4 Motor speed during light load start-up

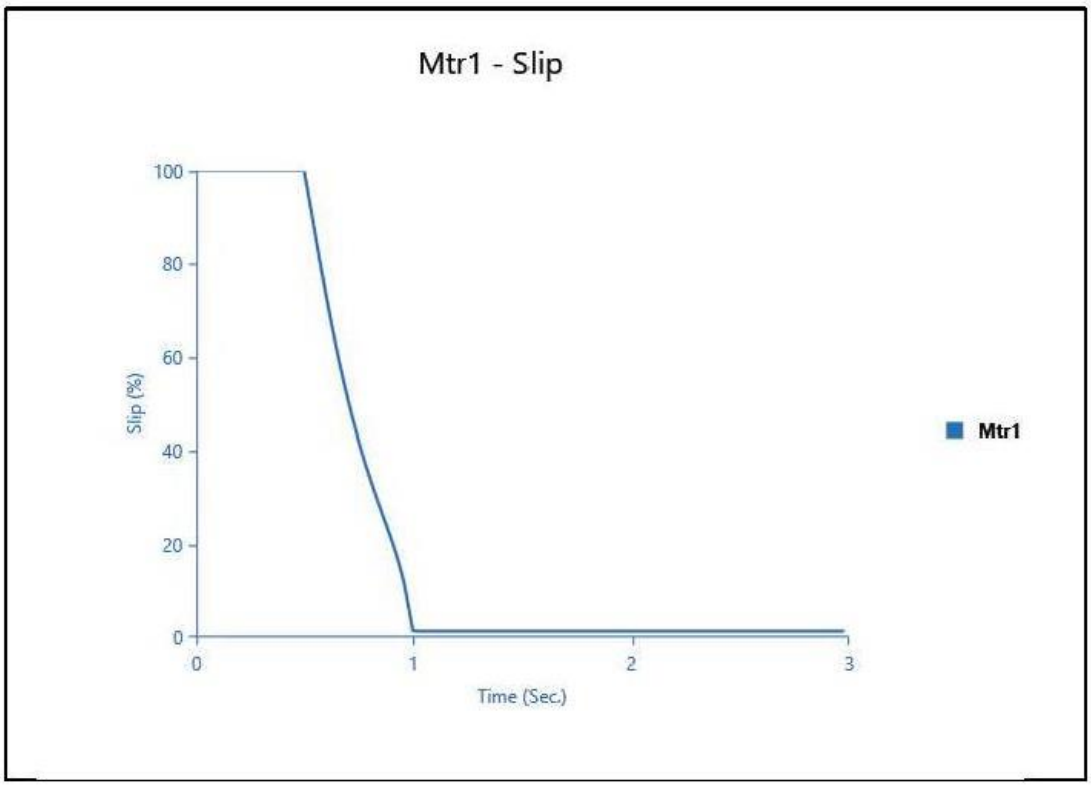


Figure A. 5 Motor slip during light load start-up

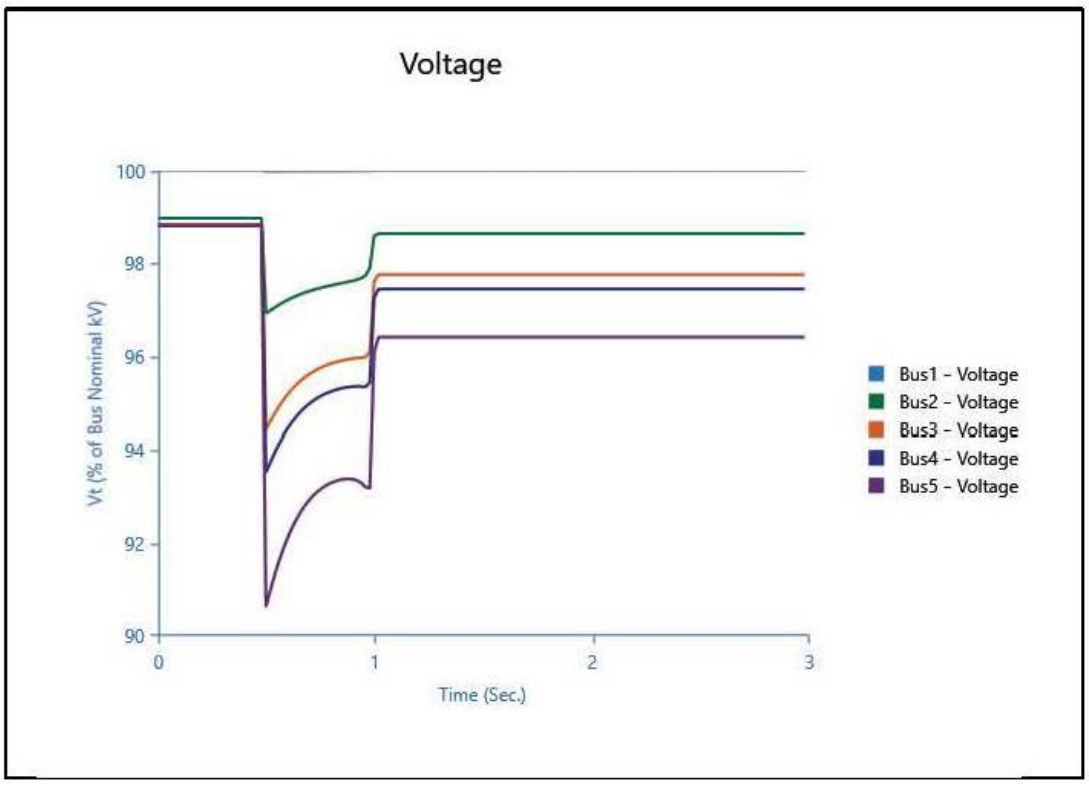


Figure A. 6 Bus voltage profiles during light load start-up

Figure A.3 illustrates the terminal current profile of the motor from its starting phase to steady state. Additionally, Figures A.4 and A.5 show the variations in the motor's speed and slip throughout the starting event under light load conditions.

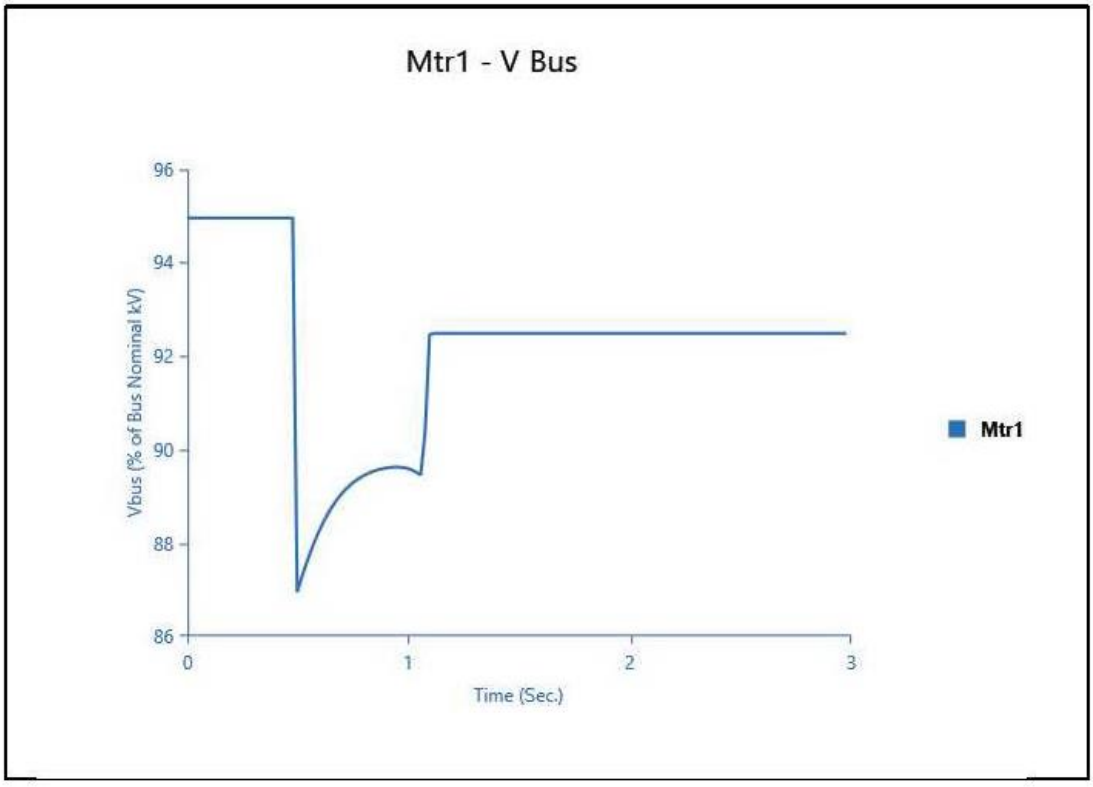


Figure A. 7 Motor PCC voltage at heavy load

These figures offer detailed insights into the motor's acceleration process from standstill to its steady state operating speed. While Figure A.6 shows motor's PCC voltage experiences no voltage sag under light load.

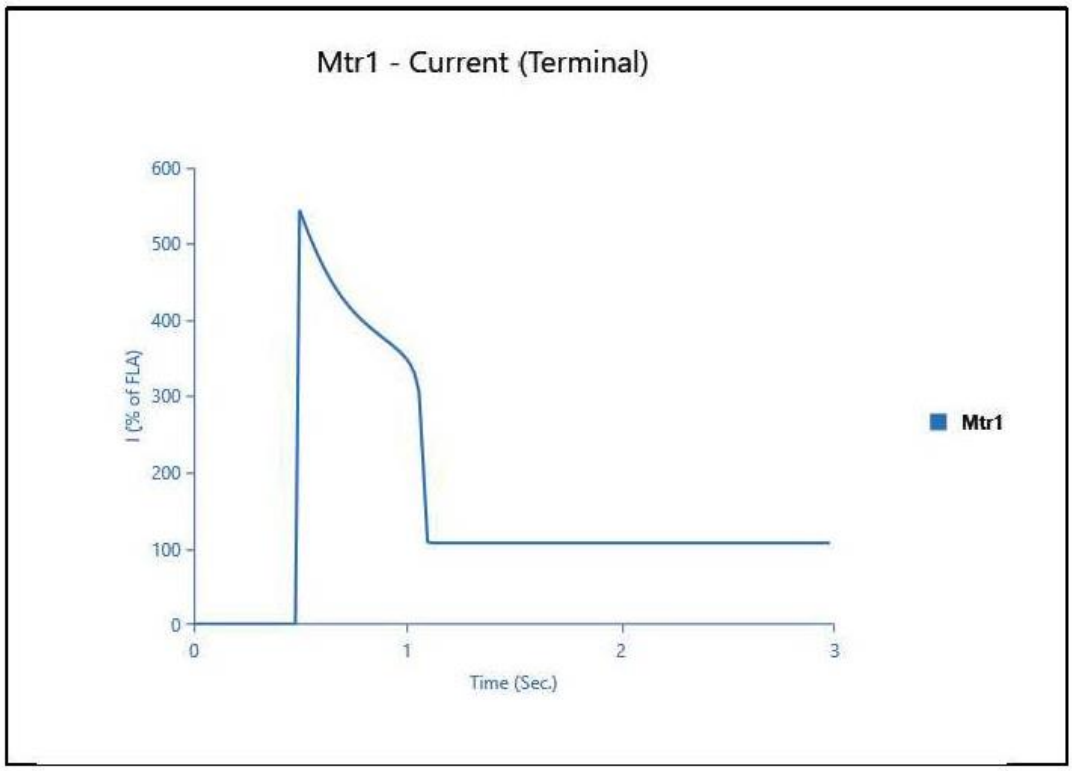


Figure A. 8 Motor terminal current during heavy load start-up

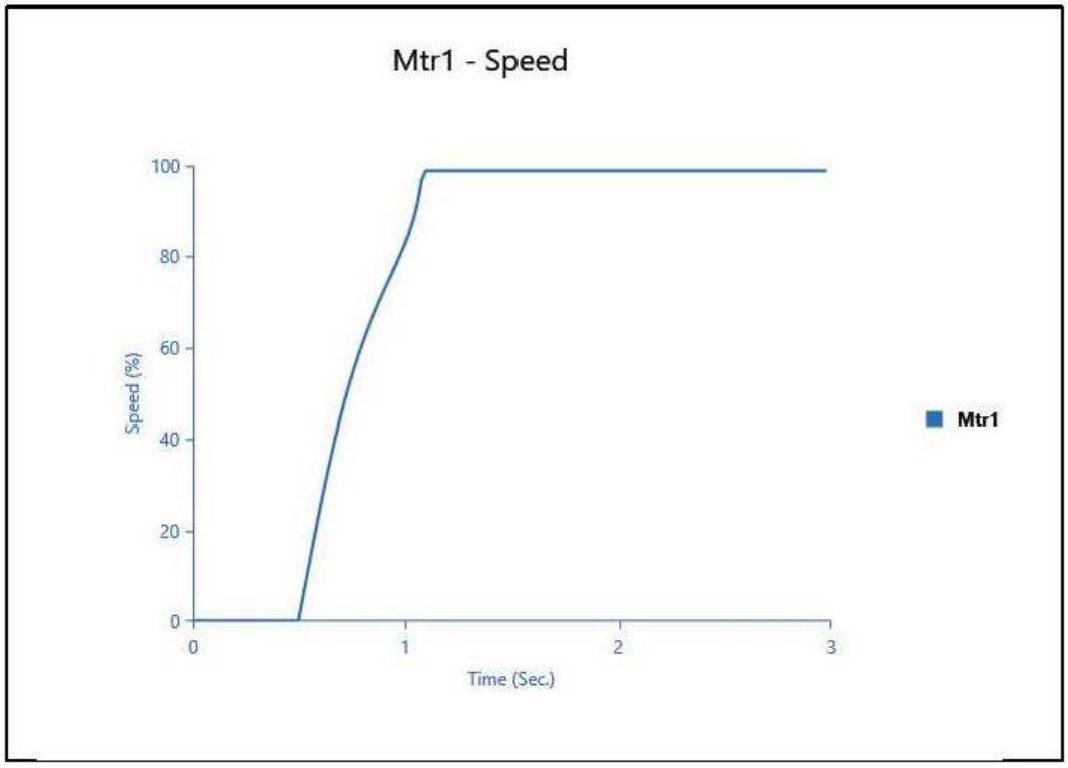


Figure A. 9 Motor speed during heavy load start-up

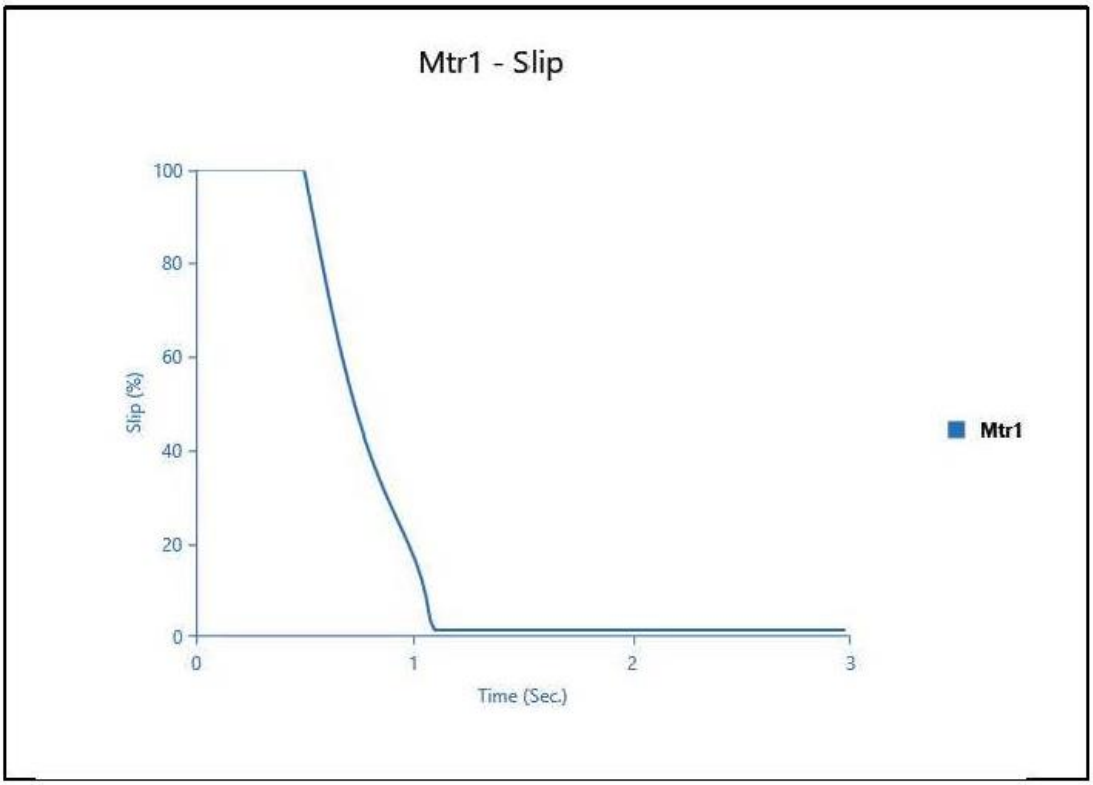


Figure A. 10 Motor slip during heavy load start-up

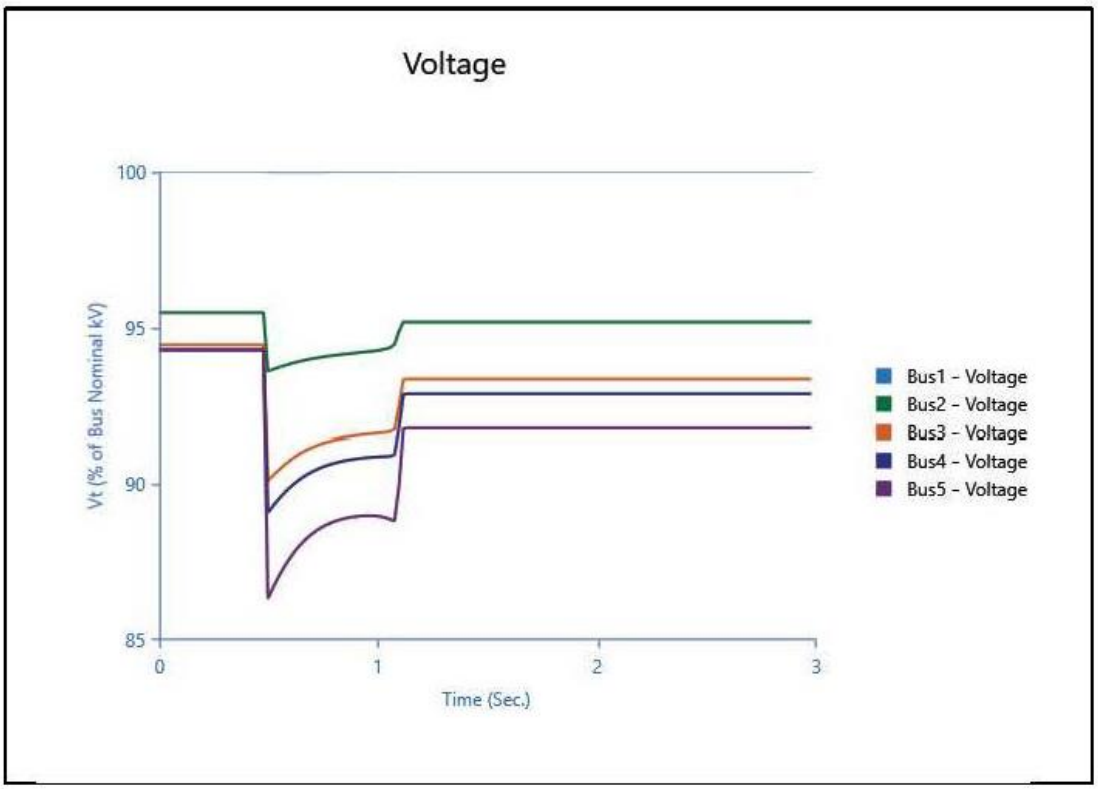


Figure A. 11 Bus voltage profiles during heavy load start-up

With the system loaded at 50% or more capacity, Figure A.7 demonstrates a considerable voltage sag at the motor's PCC during the starting event. This highlights the dependence of voltage sag severity on the system's loading conditions.

Figure A.8 shows the motor current profile during the starting event under heavy load. Figures A.9 and A.10, respectively, present the motor's speed and slip variations during the starting event under heavy load conditions.

The impact of the large machine starting event extends beyond the motor's PCC. Figure A.11 shows the voltage variations at various buses during the starting event under heavy load conditions. Notably, the figure reveals a more severe voltage sag at Bus 5, which is the bus directly connected to the motor. This finding emphasizes the need for mitigation strategies to address potential voltage sag issues during large motor starting events, particularly under heavier loading conditions.